Published in Molecular Cancer Therapeutics,
volume 17, Issue 10, pp. 2187–2196, 2018

A Chemosensitivity Study of Colorectal Cancer Using Xenografts of Patient-Derived Tumor Initiating Cells

Hisatsugu Maekawa[1, 2, *], Hiroyuki Miyoshi[1, 3, *], Tadayoshi Yamaura[1, 2], Yoshiro Itatani[1, 2], Kenji Kawada[2], Yoshiharu Sakai[2], and M. Mark Taketo[1, 3]

Authors' affiliations:

[1]Division of Experimental Therapeutics, Graduate School of Medicine, Kyoto University, Yoshida-Konoé-cho, Sakyo-ku, Kyoto 606-8501, Japan

[2]Department of Surgery, Graduate School of Medicine, Kyoto University, Shogoin-Kawahara-cho, Sakyo-ku, Kyoto 606-8507, Japan

[3]Office of Society-Academia Collaboration for Innovation, Kyoto University, Yoshida-Honmachi, Sakyo-ku, Kyoto 606-8501, Japan

* These authors contributed equally to this work.

Running title:

Chemosensitivity study of colon cancer using TIC xenografts

Key words: colorectal cancer, personalized therapy, spheroid, patient-derived xenograft, *in vivo* screening

Corresponding author: Makoto Mark Taketo, MD, PhD.
Division of Experimental Therapeutics, Graduate School of Medicine, Kyoto University, Yoshida-Konoé-cho, Sakyo-ku, Kyoto 606-8501, Japan.
Phone: 81-75-753-4391; Fax: 81-75-753-4402
E-mail: taketo@mfour.med.kyoto-u.ac.jp

Disclosure of Potential Conflicts of Interest:

The authors declare no potential conflicts of interest.

Word count: 4907; The total number of Figures; 5 and Tables; none

Abstract:

Current genomic and gene expression analyses provide versatile tools to improve cancer chemotherapy. However, it is still difficult to predict whether each patient responds to a particular regimen or not. To predict chemosensitivity in each colorectal cancer patient, we developed an evaluation method using the primary tumor initiating cells (TIC, aka cancer stem cells) xenografted in nude mice subcutaneously (patient-derived spheroid xenografts; PDSXs). Simultaneously, we also prepared the conventional patient-derived xenografts (PDXs) from the same patients' tumors, and compared the dosing results with those of PDSXs. We further compared the chemosensitivities of PDSXs with those of seven patients who had been given regimens such as FOLFOX and FOLFIRI to treat their metastatic lesions. As the results, the PDSX method provided much more precise and predictable tumor growth with less variance than conventional PDX, although both retained the epithelial characteristics of the primary tumors. Likewise, drug-dosing tests showed essentially the same results in PDXs and PDSXs, with stronger statistical power in PDSXs. Notably, the cancer chemosensitivity in each patient was precisely reflected in that of the PDSX mice along the clinical course until the resistance emerged at the terminal stage. This "paraclinical" xenograft trials using PDSXs may help selection of chemotherapy regimens efficacious for each patient, and more importantly, avoiding inefficient ones by which the patient can lose precious time and QOL. Furthermore, the PDSX method may be employed for evaluations of off-label uses of cancer chemotherapeutics and compassionate uses of yet-unapproved new drugs in personalized therapies.

Introduction

Colorectal cancer is one of the commonest types of cancer worldwide, with ~50,000 deaths estimated in 2017 (1). Although cytotoxic and molecular-targeted drugs have improved the patient survival, it is still challenging to treat metastatic colorectal cancer. For example, the overall 5-year survival rate of stage IV patients is only 13% in the U.S. (2). Because response to a regimen varies widely depending on each patient, personalized optimization of chemotherapy is important not only to give efficacious regimens but also to avoid ineffective ones.

Recently, the patient-derived tumor xenograft (PDX) mice have been adopted as a preclinical model because they preserve the genetic profiles and heterogeneity in the primary tumors (3, 4) although some caveats remain (5). Notably, drug dosing tests with PDX mice have successfully predicted chemosensitivities of the corresponding patient tumors (6, 7). However, only limited numbers of successful cases have been reported on PDX-guided personalized therapies apparently due to the long time and high cost required (3, 8).

Lately, patient-derived tumor-initiating cells (TICs, aka cancer stem cells) have been cultured *in vitro* as organoids/spheroids (9–12). These cells retain genetic and morphological characteristics of their original tumors when propagated *in vitro* (9, 10). However, these cells behave differently *in vitro* compared with those *in vivo* surrounded by tumor microenvironments that can affect chemosensitivities (13). Thus, mouse xenograft models appear to be more reliable in predicting the patient chemosensitivities. Although

patient-derived TIC spheroids can form xenograft tumors in immunocompromised mice (10, 12, 14), it remains to be evaluated whether such xenografts can serve as personalized chemosensitivity tests.

In the present study, we have established a panel of patient-derived spheroid xenografts (PDSXs) by engrafting colorectal cancer TIC spheroids subcutaneously into nude mice. We then compared them with the conventional PDXs derived from the same tumor cohort regarding the efficiency of tumor formation, time line for drug sensitivity tests, and their drug responses. Finally, we compared chemosensitivities of PDSXs with those of the corresponding patients along their clinical courses in a retrospective manner.

Materials and Methods

Human samples

Human colorectal cancer samples were obtained from patients who underwent resection operations at Kyoto University Hospital (9). The study protocol was approved by the Ethics Committee of Kyoto University, and written informed consents were obtained from the patients.

Animals

Four- to six-week-old female nude (BALB/c-nu) and NOD-SCID mice were purchased from CLEA Japan or Charles River. All animal experiments were conducted according to the protocol approved by the Animal Care and Use Committee of Kyoto University (IACUC): Title of the protocol, "Chemosensitivity studies of gastrointestinal cancers using patient-derived tumor xenografts." Approval No. 14546, 15091, 16047, 16654, 17086, and 18080 (2014–2018).

Preparation of tumor samples

Collected tumor samples were transferred from the operation room to the laboratory in the ice-cold washing medium (9) and washed with the medium and PBS twice each. Necrotic tissues were removed, and each tumor sample was cut into small cubic fragments (50–100 mm^3). One or two of them were used to establish primary cancer spheroids, and others for PDXs.

Author Manuscript Published OnlineFirst on July 3, 2018; DOI: 10.1158/1535-7163.MCT-18-0128
Author manuscripts have been peer reviewed and accepted for publication but have not yet been edited.

Tumor engraftment in patient-derived xenografts (PDXs)

To establish the founder PDXs (P_0 generation), the tumor fragments were implanted directly to each flank of nude mice and/or NOD-SCID mice under isoflurane anesthesia. The tumor size was measured and the tumor volume was estimated using the following formula; tumor volume (mm^3) = [length (mm) × width^2 (mm^2)] / 2 (15, 16).

Graft implantation was judged as successful when estimated tumor volume reached ~1000 mm^3, whereas as failed if no visible tumor mass was recognized for six months. To passage the tumors *in vivo*, we excised and cut them into smaller cubes (50–100 mm^3).

Patient-derived cancer-spheroid culture

Patient-derived colorectal cancer TIC spheroids were cultured as reported previously (9). In short, fragments of excised tumor were minced and digested by collagenase type I (Thermo Fisher Scientific). Then, epithelial cells were collected and suspended in Matrigel (Corning Inc.), and cultured in the cancer medium (9) with or without 50 ng/ml EGF (Peprotech) and 100 ng/ml basic FGF (Peprotech).

Generation of patient-derived spheroid xenografts (PDSXs)

To prepare the PDSX mice, TIC spheroids were cultured in 3 wells of a 12-well cell-culture plate for injection into a mouse. Spheroids in confluent culture (1–9 × 10^5 cells) were rinsed with PBS twice, and transferred to a 1.5-ml tube together with Matrigel.

Author Manuscript Published OnlineFirst on July 3, 2018; DOI: 10.1158/1535-7163.MCT-18-0128
Author manuscripts have been peer reviewed and accepted for publication but have not yet been edited.

Spheroid suspensions were adjusted to the total volume of 100 µl each with PBS, and injected into nude mice subcutaneously. The tumor size was measured weekly.

Histological examinations

Paraffin-embedded tissues of PDXs and PDSXs were prepared according to the standard procedures. Primary colorectal cancer sections were obtained from Department of Diagnostic Pathology, Kyoto University Hospital. Sections were stained with H&E or immunostained for MUC2 (Dako, M7313), or CDX2 (BioGenex, AM392-5M).

Chemicals

Oxaliplatin (Wako, 152-02693), irinotecan (Wako, 091-06651), 5-fluorouracil (Wako, 064-01403), and levofolinate calcium (Wako, 035-22871) were prepared in 5% glucose solution. Cetuximab (Erbitux, Merck) was diluted with PBS.

Drug sensitivity tests in mice

Groups of PDX (P_2–P_4) and PDSX mice were prepared, and subjected to drug-dosing tests when estimated tumor volume reached 300–500 mm^3. We excluded the following kinds of tumors from the tests as outliers; too small (< 100 mm^3), too large (> 900 mm^3), abscess-like, naturally shrinking, or those deeply implanted and difficult to be measured.

Mice in each set were distributed into the control and treatment groups (n = 3–6 per group). The day of the dosing start was defined as day 1, with the tumor volume and the

Author Manuscript Published OnlineFirst on July 3, 2018; DOI: 10.1158/1535-7163.MCT-18-0128
Author manuscripts have been peer reviewed and accepted for publication but have not yet been edited.

body weight of each mouse measured twice a week for 3 weeks (days 1–22).

The treatment protocols were designed to reflect clinical regimens, and drug doses for mice were calculated according to the following formula; mouse dose (mg/kg) = human dose (mg/kg) × 37 (hK_m) / 3 (mK_m) where K_m indicates human (h) or mouse (m) body surface coefficient (17).

For FOLFOX-like treatment, mice were injected intraperitoneally (i.p.) with oxaliplatin (12 mg/kg) and levofolinate calcium (30 mg/kg) first, followed by 5-fluorouracil (55 mg/kg), weekly for 3 weeks. For irinotecan treatment, mice were injected (i.p.) at 40 mg/kg weekly for 3 weeks. For FOLFIRI-like treatment, mice were injected (i.p.) with irinotecan (40 mg/kg) and levofolinate calcium (30 mg/kg) first, followed by 5-fluorouracil (55 mg/kg), weekly for 3 weeks. For cetuximab treatment, mice were injected (i.p.) at 250 μg per mouse, twice a week for 3 weeks (18). These were less than the maximal tolerated doses, and approximately 80% of the clinically relevant doses.

The relative tumor volume was obtained by calibration to the initial tumor volume on day 1. To evaluate effects of drug dosing, the T/C (Treated/Control) and TGI (Tumor Growth Inhibition) values were calculated according to the following formula (7, 16);

T/C (%) = relative tumor volume (treated) / relative tumor volume (control) × 100.

TGI (%) = [1 – Δ relative tumor volume (treated)/Δ relative tumor volume (control)] × 100, or = [1 – Δ relative tumor volume (treated)] × 100 for Δ relative tumor volume (treated) when < 0 (i.e., tumor regression),

Author Manuscript Published OnlineFirst on July 3, 2018; DOI: 10.1158/1535-7163.MCT-18-0128
Author manuscripts have been peer reviewed and accepted for publication but have not yet been edited.

□□□□□ Δ relative tumor volume = (relative tumor volume on day 22) – (relative tumor volume on day 1).

Statistical data analysis

Chi-square analyses, unpaired *t*-test, Tukey's multiple comparisons, Sidak's multiple comparisons, Spearman's correlation analyses, and Pearson's correlation analyses were performed using GraphPad Prism ver.6 (GraphPad software. Inc.)

Results

Clinical statuses of colorectal cancer patients, tumor take rates for PDXs and establishment rates for TIC spheroids *in vitro*

We collected 92 fresh colorectal cancer samples from 89 patients who underwent resection operations at Kyoto University Hospital. Background characteristics of the patients and tumors are summarized in Supplementary Table S1. We successfully established the founder generation (P_0) PDXs in 56 of 92 tumors (61%), and the TIC spheroids in 68 of 92 cases (74%). For 44 tumors, we generated both PDXs and TIC spheroids.

As reported (19), we found a correlation between advanced tumor stages and high success rates for P_0 PDXs. Namely, stage II, III, and IV tumors had higher PDX take rates (57%, 71%, and 67%, respectively) than stage I (29%). Notably, the success rates in culturing TIC spheroids were higher than the PDX take rates through all stages (Supplementary Table S1).

Histopathologically, 86 of 92 colorectal tumors (93%) analyzed here were classified as well- or moderately differentiated adenocarcinomas (i.e., low grade in a two-tiered classification) (20). The remaining six included two poorly differentiated and four mucinous adenocarcinomas. This distribution of histopathological subtypes is similar to that of common clinical cases (21). Interestingly, the latter two subtypes that are generally known as more malignant than low grade adenocarcinomas showed rather high success rates for both PDXs and PDSXs (Supplementary Table S1).

Author Manuscript Published OnlineFirst on July 3, 2018; DOI: 10.1158/1535-7163.MCT-18-0128
Author manuscripts have been peer reviewed and accepted for publication but have not yet been edited.

While 10 of 92 (11%) cases had been treated by neoadjuvant chemotherapies in this patient cohort, the success rates were not affected substantially in establishing either PDXs or spheroids by the chemotherapies (Supplementary Table S1).

In short, we procured collections of both *in vivo* PDXs and *in vitro* TIC spheroids from a cohort of colorectal cancer patients.

Establishment of patient-derived spheroid xenograft (PDSX) mice

To determine the efficiency in preparing xenografts from our TIC spheroids, we injected nude mice with 21 spheroid lines subcutaneously, and successfully developed tumors of 18 lines (at the rate of 86%) (Supplementary Table S2). We coined these xenografts as PDSXs (patient-derived spheroid xenografts) to distinguish them from the conventional PDXs.

For drug-dosing tests with PDXs, it required serial *in vivo* transplantations (more than two passages) to prepare a large number of PDX mice. In contrast, the whole set of PDSX mice could be established simultaneously once the spheroid cultures were expanded *in vitro* (5–20 passages). Overall, the cumulative success rate for PDXs was estimated to be ~43% whereas that for PDSXs was 64% (Supplementary Fig. S1). These results indicate that the PDSX method is more efficient than the conventional PDX.

PDSXs retain histopathological characteristics of original tumors

To investigate whether the PDSXs retain the primary tumor morphology, we

compared histopathology of PDSXs with that of the primary tumors and PDXs. Notably, their epithelial characteristics such as gland formation and cell differentiation were essentially identical to those of the primary tumors and PDXs for the respective cases (Supplementary Fig. S2) although mice formed less tumor stroma than humans as reported (15). Likewise, primary tumor expression of markers such as CDX2 and MUC2 was also reproduced in PDSXs (Supplementary Fig. S2).

PDSXs show smaller variances in tumor growth than PDXs

In PDXs, not all engrafted tumor fragments expanded, which was likely caused by tumor tissue heterogeneity regarding the TIC contents. Notably, PDSXs showed much smaller variances in tumor volume among individual xenografts than PDXs, despite that they derived from the same primary tumors (Supplementary Fig. S3). The mean coefficients of variation (CVs; SD divided by the mean value) for PDSXs and P_1 PDXs were 0.29 and 0.53, respectively ($P < 0.05$). The large CVs in PDXs (especially, in early passages) were problematic in the preparation of PDX mice for drug sensitivity tests. With PDSXs, on the other hand, the low CVs increased the statistical power in drug-dosing tests even with relatively small number of host mice (e.g., $n = 3$–4 per group; ref. 22). Accordingly, we concluded here that the PDSX model was more efficient and therefore suitable for drug efficacy evaluation than the conventional PDX.

PDSX mice provides more reliable results in drug sensitivity tests than PDX

Author Manuscript Published OnlineFirst on July 3, 2018; DOI: 10.1158/1535-7163.MCT-18-0128
Author manuscripts have been peer reviewed and accepted for publication but have not yet been edited.

To compare the reliability in drug-dosing tests between PDX and PDSX models, we prepared test mice transplanted with samples from four colorectal cancer patients (Fig. 1A). We had to exclude 23 of 94 (24%) PDXs as outliers because of the large individual variances in growth rates described above. On the other hand, we eliminated only 9 of 85 (11%) PDSXs according to the same criteria as applied to PDXs.

As the first example of drug dosing, we used groups of PDXs and PDSXs derived from a colon cancer case (HC13T) that turned out to carry heterozygous *BRAF*^{V600E} mutation. As anticipated, the results of drug sensitivity tests showed that cetuximab (an anti-EGFR Ab) treatment was ineffective in both PDX and PDSX mice (T/C = 120% and 114% with PDXs and PDSXs, respectively) (Fig. 1B and C, and Supplementary Table S3). On the other hand, a FOLFOX-like regimen significantly decreased the tumor growth (T/C = 48% and 57% with PDXs and PDSXs, respectively) (Fig. 1B and C, and Supplementary Table S3). Notably, PDXs showed much larger variances in tumor growths than PDSXs even the outliers had been eliminated before dosing (Fig. 1B and C, and Supplementary Table S4). Accordingly, the dosing data with PDSXs led to stronger statistical differences than those with PDXs (Fig. 1B and C). Essentially the same results were obtained with tumors from three additional patients (Supplementary Fig. S4, Supplementary Tables S3 and S4). Regarding therapy responses, the mean values for PDSXs correlated well with those for PDXs (in T/C and TGI, Spearman's correlation; R = 0.67 and 0.90, respectively) (Supplementary Table S3). These results indicate that the difference between PDSXs and PDXs did not affect drug sensitivities substantially. Importantly, however, all data sets of

PDSXs had only half as large CVs as those of PDXs with a significant statistical difference (the mean CVs were 19% and 31% for PDSXs and PDXs, respectively, $P < 0.01$) (Supplementary Table S4).

To ensure the reproducibility of the two methods, we performed drug sensitivity tests of HC13T xenografts with independently prepared additional set of both PDXs and PDSXs. Notably, the first and second set relative tumor volumes of PDSXs were almost identical between the corresponding test groups (e.g., Control 1 and 2 *in* Fig. 2C and D). However, those of PDXs showed much wider variances (e.g., Control 1 and 2 *in* Fig. 2A and B). In addition, there was a statistically significant difference between the mean tumor volumes of PDX Cetuximab 1 and 2 data ($P < 0.01$) (Fig. 2A and B). We obtained similar results with tumors from two more patients (HC5T and HC17T), underscoring higher reproducibility of the PDSX model than PDX (Supplementary Fig. S5).

Thus, the PDSX method enabled us to decrease individual variances in xenograft growth rates and to evaluate colorectal cancer chemosensitivity even with such small numbers of mice as three to four in each dosage group.

Drug sensitivity in PDSXs reflects clinical outcome of colorectal cancer patients

To exploit PDSXs for personalized treatments, we compared drug responses of PDSXs with those of the patients in a retrospective manner. We prepared panels of PDSXs from seven patients who had been treated with several chemotherapeutic regimens for liver or peritoneal metastasis after resection of their primary colorectal cancers. We performed a

total of nine drug-dosing tests that matched the regimens given to the corresponding patients (Supplementary Table S5). The clinical courses for three individual patients are summarized below (Figs. 3–5), and four more are presented in (Supplementary Figs. S6–9):

Patient 1 (HC1T; Fig. 3). This patient was treated by S-1 (a 5-FU prodrug) + oxaliplatin (i.e., a FOLFOX-like regimen) for the metastatic lesions, which led to an SD (stable disease) (Fig. 3A, B-b and B-c). In PDSX mice, a FOLFOX-like dosing caused a moderate response with a significant difference from the control group (T/C = 50%, TGI = 82%; $P < 0.01$) (Fig. 3C and Supplementary Table S5). Thereafter, the patient was treated with irinotecan + cetuximab, which resulted in another SD (Fig. 3A, B-d and B-e), although the treatment was interrupted for a month due to an accidental knee bone fracture (Fig. 3A). When we performed the same irinotecan + cetuximab regimen on the PDSX mice, it caused a moderate suppression of tumor growth, indicating that the primary tumor was responsive to this therapy (T/C = 37%, TGI = 93%; $P < 0.01$) (Fig. 3D and Supplementary Table S5). Accordingly, both sets of these clinical responses in this patient to the regimens were reproduced well in the PDSX dosing experiments.

Patient 2 (HC6T; Fig. 4). This patient was treated with FOLFOX + panitumumab (an anti-EGFR antibody) regimen that caused dramatic decreases in the tumor volume (PR, partial response) and serum CEA level (Fig. 4A, B-b and B-c). Following the post-operative FOLFOX + panitumumab treatment, he was switched to FOLFIRI + bevacizumab regimen. Although the treatment led to a condition evaluated as an SD at first, the CEA level was increasing steadily and the size of metastatic lesions increased during six

months of treatment (Fig. 4A, B-c and B-d). In the PDSX model, transplanted tumors were sensitive to FOLFOX + cetuximab (T/C = 42%, TGI = 122%; $P < 0.01$) (Fig. 4C, D and Supplementary Table S5). On the other hand, they did not respond to the FOLFIRI regimen well (T/C = 76%, TGI = 50%; $P < 0.05$) (Fig. 4C, D and Supplementary Table S5). Accordingly, the marginal effects of the FOLFIRI-based treatment for the patient appeared to be an innate characteristic of the primary cancer, which was reflected in the PDSX data.

Patient 3 (HC50T; Fig. 5). On the other hand, there was only one set of PDSX drug-dosing results that did not appear to match with the clinical evaluation (RECIST) of a chemotherapy regimen. In this case, the patient was treated by (FOLFIRI-like) S-1 + irinotecan + bevacitumab regimen. The efficacy of S-1 + irinotecan regimen was clinically assessed as a PD (progressive disease) with a 21% increase in the metastatic tumor volume determined by MRI during the treatment (Fig. 5A, Fig. 5B-a and B-b). Despite the clinical assessment of PD above, the PDSXs treated with FOLFIRI were reduced in size significantly (T/C = 55%; TGI = 107%; $P < 0.05$) (Fig. 5C, D and Supplementary Table S5).

Upon close re-examination of the clinical course (Fig. 5A), the above assessment was likely affected by the timing of MRI examinations. Consistent with the sharply decreased levels of CEA and CA19-9 after the overshoots that were caused by resistance to the preceding chemotherapy with XELOX (Fig. 5A), the results of ^{18}F-FDG–PET images taken one month after the respective MRI photos showed markedly reduced liver glucose metabolism in the metastatic lesions (compare Fig. 5B-c and B-d). Even if the S1 +

Author Manuscript Published OnlineFirst on July 3, 2018; DOI: 10.1158/1535-7163.MCT-18-0128
Author manuscripts have been peer reviewed and accepted for publication but have not yet been edited.

irinotecan + bevacitumab regimen was efficacious, it was likely to have taken some time before the metastatic tumors shrunk to the volume smaller than that in the previous MRI. In sum, the apparent discrepancy between one of the clinical assessments and PDSX results was of the transitional nature during the clinical course, and therefore did not discredit the PDSX evaluation method.

Accordingly, all nine sets of the drug-dosing results with PDSXs well reflected their corresponding clinical outcome (Supplementary Table S5). Namely, the therapeutic regimens that were efficacious in the patients (PR or SD by RECIST) were also effective in treating PDSXs (Supplementary Table S5). In addition, there were strong correlations between the results of PDSX dosing tests (T/C) and patient outcome, as well as those and DOR (Supplementary Fig. S10A and B). Correlations were also confirmed between TGI and the patient outcome as well as DOR (Supplementary Fig. S10C and D).

Taken together, these results support the robust reliability of PDSXs in "paraclinical" evaluation of chemosensitivity (see Discussion).

PDSX method can expedite drug sensitivity tests compared with PDX

One of the most practical limitations of the PDX method for personalized medicine is the long and unpredictable time it takes to prepare enough numbers of PDX mice for drug-dosing tests. For example, it took five months or longer to set up a group of P_2 generation PDXs in our study. Thereafter, it took ~35 days for P_2 PDXs to expand to the size of 300–500 mm^3 (i.e., appropriate for drug-dosing) (Supplementary Fig. S11, top). In

Author Manuscript Published OnlineFirst on July 3, 2018; DOI: 10.1158/1535-7163.MCT-18-0128
Author manuscripts have been peer reviewed and accepted for publication but have not yet been edited.

contrast, it took us only 2–3 months to prepare a group of ~20 PDSX mice (Supplementary Fig. S11, bottom). These results indicate that the PDSX method is more advantageous than PDX not only in the accuracy of drug sensitivity testing but also in saving time for preparation of the tumor-bearing mice. Accordingly, it should be easier to feedback the dosing data to the bedside before deterioration of the patient conditions.

Discussion

The present results demonstrate three advantages of PDSXs over conventional PDXs in clinical application to chemosensitivity tests. First, the PDSX method showed a higher efficiency (i.e., take rate) than the conventional PDX method in the dosing-test mouse preparation, which should provide the personalized clinical services to a wider cohort of colorectal cancer patients. The take rates for conventional PDXs were reported as 60–80% at the founder generation (3, 4), although the tumor take was not always defined precisely (23). The cumulative rate after three passages of colorectal cancer was reported to be 43% in nude mice (24), which is similar to the present results (43%; from primary tumors to P_1 PDXs). Only a few pieces of data were reported on the tumor take rate regarding spheroids/organoids injected into immunodeficient mice (14, 25). In this study, we established TIC spheroid lines for 74% (68/92) of primary tumors and generated PDSX mice for 86% (18/21) of the spheroid lines. One of the reasons for this high success rate of PDSX formation was likely because we expanded TICs in culture and thereafter injected them in larger numbers than those contained in the PDX transplants. Regarding intratumor heterogeneities, our PDXs and spheroids that derived from separate subregions of the same tumor were almost identical as others reported (5, 26, 27).

Second, the PDSX method allowed us to reduce variances in the tumor growth rate. As noted above, TIC spheroids consisted of only proliferating cancer epithelial cells. In case of PDXs, on the other hand, the engrafted tumor fragments upon passages were likely to be heterogeneous regarding the number of live TICs and their microenvironment (e.g.,

the extent of differentiation and co-existing stromal cells, respectively). In fact, we had significantly fewer mice excluded in the PDSX groups than in PDX upon preparations for drug-dosing tests, indicating that PDSX method is less wasteful in xenograft formation.

Third, and most importantly, PDSXs gave chemosensitivity data statistically more significant than PDXs in drug-dosing tests. Accordingly, it is expected that the clinical responses can be predicted more reliably with PDSX mice than with PDX. To date, many methods have been proposed that predict patient responses to cancer chemotherapeutics (28). These include mutational analyses, gene expression signature analyses, as well as *in vitro* sensitivity tests with cancer organoids similar to spheroids (14, 29). For example, colorectal cancer that retains intact Ras signaling with wild-type *RAS* genes responds to EGFR inhibitors at a high probability (25, 30). However, there is always a sizable fraction in the patient population that does not respond to the indicated regimen(s). Although it is beneficial to each patient if a regimen is efficacious, the patient will lose precious time and QOL if not. Thus, more reliable prediction methods are awaited. To this end, direct tumor grafts to immunodeficient mice (i.e., PDXs) have been proposed as a straightforward method of drug sensitivity evaluation personalized to the respective patients (3, 4).

Our present results provide a rationale for PDSXs as a more improved method than PDXs, overcoming the drawbacks of the latter. Namely, the results of PDSX drug-dosing tests demonstrated a strong correlation with the clinical responses (Figs. 3–5; Supplementary Figs. S6–9), and paralleled with those of PDXs (Supplementary Table S3). Therefore, these results suggest a strong predictive power in chemosensitivity when applied

to personalized prospective studies. To this end, our PDSX method also helps expedite preparation of test mice for drug-dosing tests. Namely, it took only 2–3 months to setup groups of PDSXs for testing several regimens. Notably, however, some types of cancer may be excluded that take very rapid downhill courses such as pancreatic cancer. It can be more practical to test the sensitivity of spheroids *in vitro* for such types. Along this line, *in vitro* cultures of spheroids/organoids have been proposed to be used in drug screening as well as in personalized chemosensitivity tests (9, 31). Such *in vitro* sensitivity tests may provide quicker, though limited, answers for a class of chemotherapeutics that directly target cancer cell proliferation. In other words, there are occasions in which xenografts can provide more practical prediction of the clinical courses as exemplified by irinotecan sensitivity in Fig. 4. While irinotecan resistance was reported to correlate with the expression level of DNA topoisomerase I (32), our expression analysis did not provide enough data that allowed personalized predictions.

Taken together, the PDSX method should allow us to design personalized chemotherapy regimens for patients with advanced colorectal cancer in a prospective manner. We would like to propose introduction of personalized PDSX-based chemosensitivity tests as “personalized paraclinical prediction” (PPP) trials. For testing already established regimens, they can be designated as PPP phase 3.5X trials (X for xenograft) because the drugs had completed phase 3 clinical trials. When the tests can be performed using *in vitro* culture of spheroids/organoids, they may be PPP phase 3.5V (V for *in vitro*). If candidate drugs for repurposing are used, they can be PPP 1.5X or 1.5V trials,

and so on. We encourage further discussion among those who participate in cancer chemotherapy development.

Notably, PDSXs have some limitations common to PDXs because both lack key immune responses and have different stromal microenvironment from that of human hosts. Technical improvements to humanize the mouse immune system and mimic the patient tumor microenvironment in mice appear to be in progress although multiple difficulties still remain (4, 33, 34). Despite such limitations, PDX has been one of the best preclinical models owing to their predictive power for a variety of chemotherapeutics (3, 4).

In conclusion, we have demonstrated that PDSXs are reliable "paraclinical" models for personalized colorectal cancer chemotherapies. Our methods of TIC spheroids and PDSXs are straightforward, reliable, and well-formulated. They also meet the time line in most colorectal cancer clinical courses. In addition, PDSXs may be applied to chemotherapies of not only colorectal cancer but also other types of cancer when the primary tumors are available. It is worth noting that applications of the PDSX method can be extended to evaluations of off-label uses of therapeutics and compassionate uses of yet un-approved drugs.

Acknowledgment We thank the Medical Research Support Center, Graduate School of Medicine, Kyoto University for the technical supports. We also thank the members of the Division of Gastrointestinal Surgery, Department of Surgery for help in

collecting surgical specimens. We are grateful to T Sakurai and H Haga of the Department of Clinical Pathology at Kyoto University Hospital for their pathological diagnosis. We are also grateful to S Matsumomo, T Horimatsu, M Kanai and M Muto of Department of Clinical Oncology, Kyoto University Hospital for clinical discussions on chemotherapy.

This work was supported by Program for Creating STart-ups from Advanced Research and Technology (START, ST261001TT) from Japan Science and Technology Agency (JST); Practical Research for Innovative Cancer Control (ck0106195h) from Japan Agency for Medical Research and Development (AMED); and Kyoto University Venture Incubation from Kyoto University Office of Society-Academia Collaboration for Innovation (to M.M.Taketo)

References

1. Siegel RL, Miller KD, Fedewa SA, Ahnen DJ, Meester RGS, Barzi A, et al. Colorectal cancer statistics, 2017. CA Cancer J Clin. 2017;67:177–93.
2. American Cancer Society. Colorectal cancer facts & figures 2014-2016. Color Cancer Facts Fig. 2014;1–32.
3. Hidalgo M, Amant F, Biankin A V., Budinská E, Byrne AT, Caldas C, et al. Patient-derived xenograft models: An emerging platform for translational cancer research. Cancer Discov. 2014;4:998–1013.
4. Byrne AT, Alferez DG, Amant F, Annibali D, Arribas J, Biankn AV et al. Interrogating open issues in cancer precision medicine with patient-derived xenografts. Nat Rev Cancer. 2015;17:254–268.
5. Ben-David U, Ha G, Tseng Y-Y, Greenwald NF, Oh C, Shih J, et al. Patient-derived xenografts undergo mouse-specific tumor evolution. Nat Genet. 2017;49:1567–75.
6. Hidalgo M, Bruckheimer E, Rajeshkumar N V, Garrido-Laguna I, De Oliveira E, Rubio-Viqueira B, et al. A pilot clinical study of treatment guided by personalized tumorgrafts in patients with advanced cancer. Mol Cancer Ther. 2011;10:1311–6.
7. Stebbing J, Paz K, Schwartz GK, Wexler LH, Maki R, Pollock RE, et al. Patient-derived xenografts for individualized care in advanced sarcoma. Cancer. 2014;120:2006–15.
8. Morton CL, Houghton PJ. Establishment of human tumor xenografts in

immunodeficient mice. Nat Protoc. 2007;2:247–50.

9. Miyoshi H, Maekawa H, Kakizaki F, Yamaura T, Kawada K, Sakai Y, et. al. An improved method for cultureing patient-derived colorectal cancer spheroids. Oncotarget. 2018;9:21950–64.

10. van de Wetering M, Francies HE, Francis JM, Bounova G, Iorio F, Pronk A, et al. Prospective derivation of a living organoid biobank of colorectal cancer patients. Cell. 2015;161:933–45.

11. Fujii M, Shimokawa M, Date S, Takano A, Matano M, Nanki K, et al. A colorectal tumor organoid library demonstrates progressive loss of niche factor requirements during tumorigenesis. Cell Stem Cell. 2016;18:827–38.

12. Kondo J, Endo H, Okuyama H, Ishikawa O, Iishi H, Tsujii M, et al. Retaining cell-cell contact enables preparation and culture of spheroids composed of pure primary cancer cells from colorectal cancer. Proc Natl Acad Sci U S A. 2011;108:6235–40.

13. Choi SYC, Lin D, Gout PW, Collins CC, Xu Y, Wang Y. Lessons from patient-derived xenografts for better in vitro modeling of human cancer. Adv Drug Deliv Rev. 2014;79–80:222–37.

14. Pauli C, Hopkins BD, Prandi D, Shaw R, Fedrizzi T, Sboner A, et al. Personalized in vitro and in vivo cancer models to guide precision medicine. Cancer Discov. 2017;7:462–77.

15. Julien S, Merino-Trigo A, Lacroix L, Pocard M, Goéré D, Mariani P, et al. Characterization of a large panel of patient-derived tumor xenografts representing the

clinical heterogeneity of human colorectal cancer. Clin Cancer Res. 2012;18:5314–28.

16. Sausville EA. Preclinical models for anticancer drug development. In: Garrett-Mayer E, editor. Princ Anticancer Drug Dev. 2011. page 89–114.

17. Reagan-Shaw S, Nihal M, Ahmad N. Dose translation from animal to human studies revisited. FASEB J. 2008;22:659–61.

18. Luo FR, Yang Z, Dong H, Camuso A, McGlinchey K, Fager K, et al. Correlation of pharmacokinetics with the antitumor activity of cetuximab in nude mice bearing the GEO human colon carcinoma xenograft. Cancer Chemother Pharmacol. 2005;56:455–64.

19. Oh BY, Lee WY, Jung S, Hong HK, Nam D-H, Park YA, et al. Correlation between tumor engraftment in patient-derived xenograft models and clinical outcomes in colorectal cancer patients. Oncotarget. 2015;6:16059–68.

20. Compton CC, Fielding LP, Burgart LJ, Conley B, Cooper HS, Hamilton SR, et al. Prognostic factors in colorectal cancer. College of American Pathologists Consensus Statement 1999. Arch Pathol Lab Med. 2000;124:979–94.

21. Fleming M, Ravula S, Tatishchev SF, Wang HL. Colorectal carcinoma: Pathologic aspects. J Gastrointest Oncol 2012;3:153-173.

22. Wu J. Statistical inference for tumor growth inhibition T/C ratio. J Biopharm Stat. 2010;20:954–64.

23. Brown KM, Xue A, Mittal A, Samra JS, Smith R, Hugh TJ. Patient-derived xenograft models of colorectal cancer in pre-clinical research: a systematic review. Oncotarget.

2016;7:66212–25.

24. Fichtner I, Slisow W, Gill J, Becker M, Elbe B, Hillebrand T, et al. Anticancer drug response and expression of molecular markers in early-passage xenotransplanted colon carcinomas. Eur J Cancer. 2004;40:298–307.

25. Schütte M, Risch T, Abdavi-Azar N, Boehnke K, Schumacher D, Keil M, et al. Molecular dissection of colorectal cancer in pre-clinical models identifies biomarkers predicting sensitivity to EGFR inhibitors. Nat Commun. 2017;8:14262.

26. Gao H, Korn JM, Ferretti S, Monahan JE, Wang Y, Singh M, et al. High-throughput screening using patient-derived tumor xenografts to predict clinical trial drug response. Nat Med. 2015;21:1318–25.

27. Bruna A, Rueda OM, Greenwood W, Batra AS, Callari M, Batra RN, et al. A Biobank of Breast Cancer Explants with Preserved Intra-tumor Heterogeneity to Screen Anticancer Compounds. Cell. The Authors; 2016;167:260–274.e22.

28. Friedman AA, Letai A, Fisher DE, Flaherty KT. Precision medicine for cancer with next-generation functional diagnostics. Nat Rev Cancer. 2015;15:747–56.

29. Calon A, Lonardo E, Berenguer-Llergo A, Espinet E, Hernando-Momblona X, Iglesias M, et al. Stromal gene expression defines poor-prognosis subtypes in colorectal cancer. Nat Genet. 2015;47:320–9.

30. Sorich MJ, Wiese MD, Rowland A, Kichenadasse G, McKinnon RA, Karapetis CS. Extended RAS mutations and anti-EGFR monoclonal antibody survival benefit in metastatic colorectal cancer: a meta-analysis of randomized, controlled trials. Ann

Oncol. 2015;26:13–21.

31. Weeber F, Ooft SN, Dijkstra KK, Voest EE. Tumor organoids as a pre-clinical cancer model for drug discovery. Cell Chem Biol. 2017;24:1092–100.

32. Hammond WA, Swaika A, Mody K. Pharmacologic resistance in colorectal cancer: a review. Ther Adv Med Oncol. 2016;8:57–84.

33. Morton JJ, Bird G, Refaeli Y, Jimeno A. Humanized mouse xenograft models: Narrowing the tumor-microenvironment gap. Cancer Res. 2016;76:6153–8.

34. Francone TD, Landmann RG, Chen C-T, Sun MY, Kuntz EJ, Zeng Z, et al. Novel xenograft model expressing human hepatocyte growth factor shows ligand-dependent growth of c-Met-expressing tumors. Mol Cancer Ther. 2007;6:1460–6.

Figure Legends

Figure 1.

Comparison between PDXs and PDSXs in drug-dosing tests.

A, Schematic comparison between PDX and PDSX chemosensitivity tests. The PDX and PDSX mice were prepared using tumor samples from the same patient. Mice with PDXs (P_2–P_3) and PDSXs were used for drug-dosing tests. Test mice were divided into three groups (control, FOLFOX, and cetuximab). Drug dosing was started on day 1 and completed on day 22. **B** and **C**, Results of drug-dosing tests with PDXs (**B**) and PDSXs (**C**). Each data point shows the tumor volume of the corresponding PDX/PDSX on day x relative to that of day 1. To help visual clarity, three data points for each day were aligned horizontally, avoiding their superimposition. Accordingly, blue (for control) and green (for cetuximab) points are slightly off the center (red for FOLFOX) although they all represent precisely the same day. (n = 5–6 in each group; Error bars show SDs. *, $P < 0.05$; **, $P < 0.01$; and n.s., not significant in Tukey's multiple comparisons)

Figure 2.

Comparison of reproducibility in drug dosing tests between PDXs and PDSXs (HC13T)

A, Results from the first (filled symbols) and second (open symbols) rounds of drug-dosing tests with PDX mice (n = 2–4 in each group). The P_2 and P_3 generation PDX mice were used for the first and second rounds of drug-dosing tests, respectively. **B,** Result of Sidak's

multiple comparison test for the corresponding test groups (e.g., Control-1 and Control-2) in two rounds of dosing tests with PDXs. **C,** Results from the first (filled symbols) and second (open symbols) rounds of drug-dosing tests with PDSX mice (n = 2–4 in each group). The PDSXs derived from P_{12} and P_{16} spheroids were used for the first and second round, respectively. **D,** Result of Sidak's multiple comparison test for the corresponding test groups with PDSXs (Error bars show SDs; **, $P < 0.01$). To help visual clarity, three data points for each day in (**A**) and (**C**) were aligned horizontally, avoiding their superimposition. Accordingly, blue (for control) and green (for cetuximab) points are slightly off the center (red for FOLFOX) although they all represent precisely the same day.

Figure 3.

Clinical course of the colon cancer patient during chemotherapies after resection of HC1T, and its drug responses as PDSXs. **A,** The serum CEA level was monitored. Chemotherapy regimens given to the patient are shown on top with colored arrows that indicate the durations. The black diamond (a) indicates an interruption of chemotherapy due to an accidental knee bone fracture. Ope, operation; Ox, oxialiplatin. C-mab, cetuximab. **B,** CT images of the patient before (b) and after (c) SOX (S-1 + Ox; similar to FOLFOX), and before (d) and after (e) irinotecan + C-mab treatment. White arrowheads point a peritoneal metastatic tumor. The best responses to SOX and irinotecan + C-mab treatment in the patient were SD (stable disease; +11% and + 3% with RECIST, respectively). **C,** Drug-dosing tests with PDSXs (derived from HC1T). The tumor growth in the FOLFOX

mice was significantly inhibited compared with that in the control group (left). Percent changes in tumor volume from individual mice with or without the dosing (right). **D,** Another drug-dosing test with PDSXs. The tumor growth in the treated (Irinotecan + C-mab) mice was significantly suppressed compared with that in the control mice (left). Percent changes in tumor volume from the individual mice with or without the dosing (right). Error bars show SEMs. ** $P < 0.01$ in unpaired *t* test on day 22.

Figure 4.

Clinical course of the colon cancer patient during chemotherapies before and after resection of HC6T, and its drug responses as PDSXs. **A,** The serum CEA level was monitored. Chemotherapy regimens given to the patient are shown on top with colored arrows that indicate the durations. The black diamond (a) indicates an interruption of chemotherapy for resection operation of the primary tumor. P-mab, panitumumab; an anti-EGFR antibody similar to cetuximab. B-mab, bevacizumab; an anti-VEGF antibody. **B,** CT images of the patient before (b) and after (c) FOLFOX + P-mab treatment, and after (d) FOLFIRI + B-mab treatment. The best response to FOLFOX + P-mab treatment in the patient was PR (partial response; -60% with RECIST). On the other hand, the best response to FOLFIRI + B-mab treatment was SD (stable disease; +10% in RECIST). **C,** Drug dosing tests with PDSXs (derived from HC6T). The tumor growth in the FOLFOX + C-mab (cetuximab) mice was significantly inhibited compared with that in the control. On the other hand, the tumor growth in the FOLFIRI mice showed only a slight and delayed decrease compared

with that in the control, which was less significant statistically than the FOXFOX + C-mab effect. (Error bars show SEM. *, $P < 0.05$; ***, $P < 0.001$ in unpaired t test. $n = 2–3$ in each group) **D,** Percent changes in tumor volume from the individual mice with or without the dosing (days 1–22).

Figure 5.

Clinical course of the patient during chemotherapies whose rectal cancer HC50T and its liver metastasis were resected simultaneously, and primary tumor drug-response as PDSXs. **A,** The serum CEA and CA19-9 levels were monitored. Chemotherapy regimens given to the patient are shown on top with colored arrows that indicate the durations. Ope, operation; Lv, liver; Lg, lung; Met, metastases; B-mab, bevacitumab. The red arrowheads (a and b) indicate the timing of MRI assessments in (**B**) whereas the blue arrowheads (c and d) point that of ^{18}F-fluorodeoxyglucose (FDG)-positron emission tomography (PET) examinations. **B,** Liver images of the patient by MRI (a and b) before (a) and after (b) S-1 + irinotecan (IRIS; similar to FOLFIRI) + B-mab treatment, and those of PET (c and d) about a month after the respective MRI examinations. The best response to IRIS + B-mab treatment in the patient was assessed as PD (progressive disease; 21%) by MRI (a and b) although the standard uptake value (SUV) of the metastatic tumors with ^{18}F-FDG-PET significantly decreased after treatment (c and d). **C,** Drug-dosing test with PDSXs derived from the primary tumor. The tumor growth in the FOLFIRI mice was significantly suppressed compared with that in the control mice. (Error bars show SEM. *, $P < 0.05$ by

unpaired *t* test on day 22. $n = 3$ in each group.) **D,** Percent changes in tumor volume from the individual PDSX mice with or without the dosing (days 1–22).

Author Manuscript Published OnlineFirst on July 3, 2018; DOI: 10.1158/1535-7163.MCT-18-0128
Author manuscripts have been peer reviewed and accepted for publication but have not yet been edited.

Figure 1

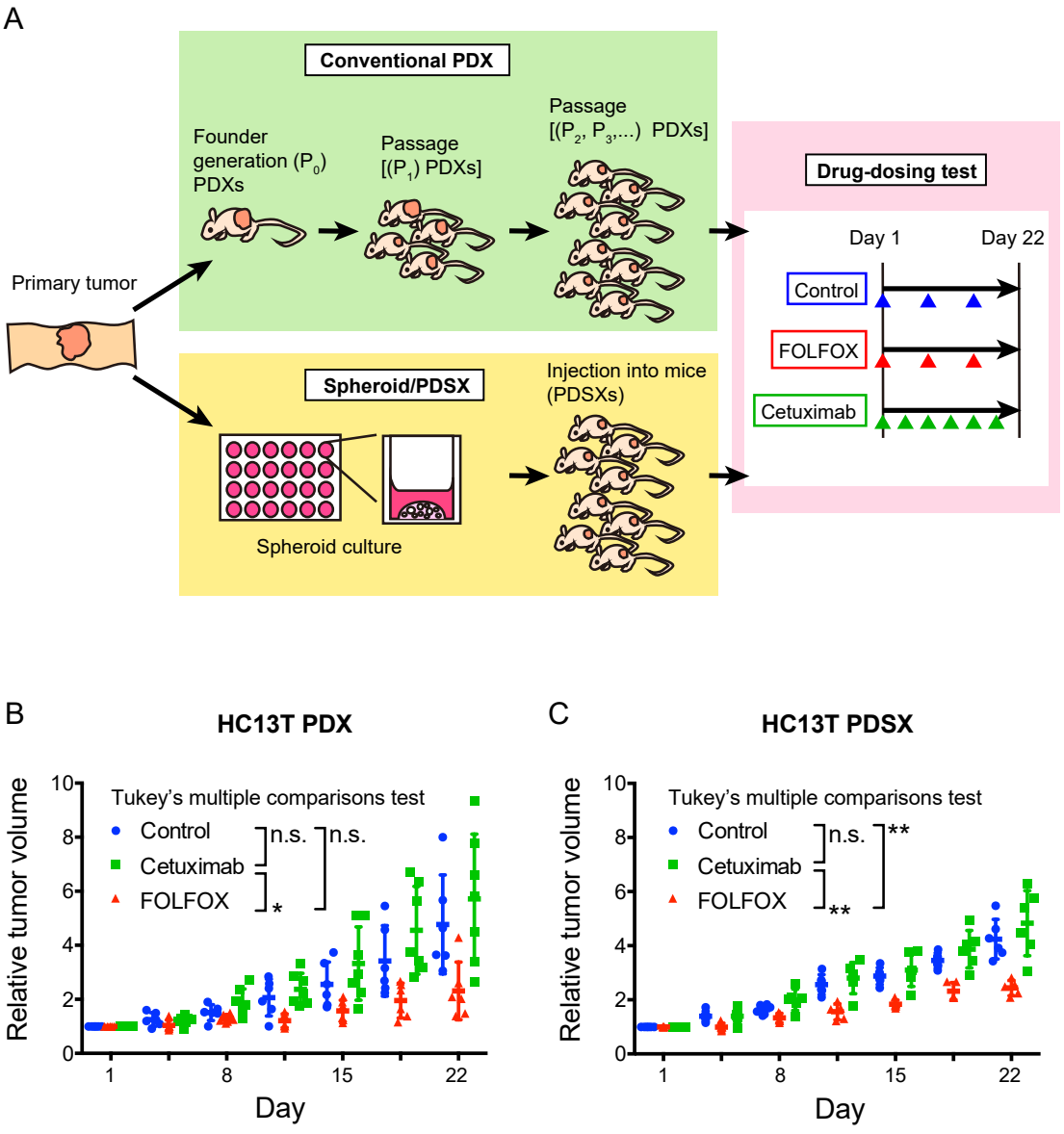

Author Manuscript Published OnlineFirst on July 3, 2018; DOI: 10.1158/1535-7163.MCT-18-0128
Author manuscripts have been peer reviewed and accepted for publication but have not yet been edited.

Figure 2

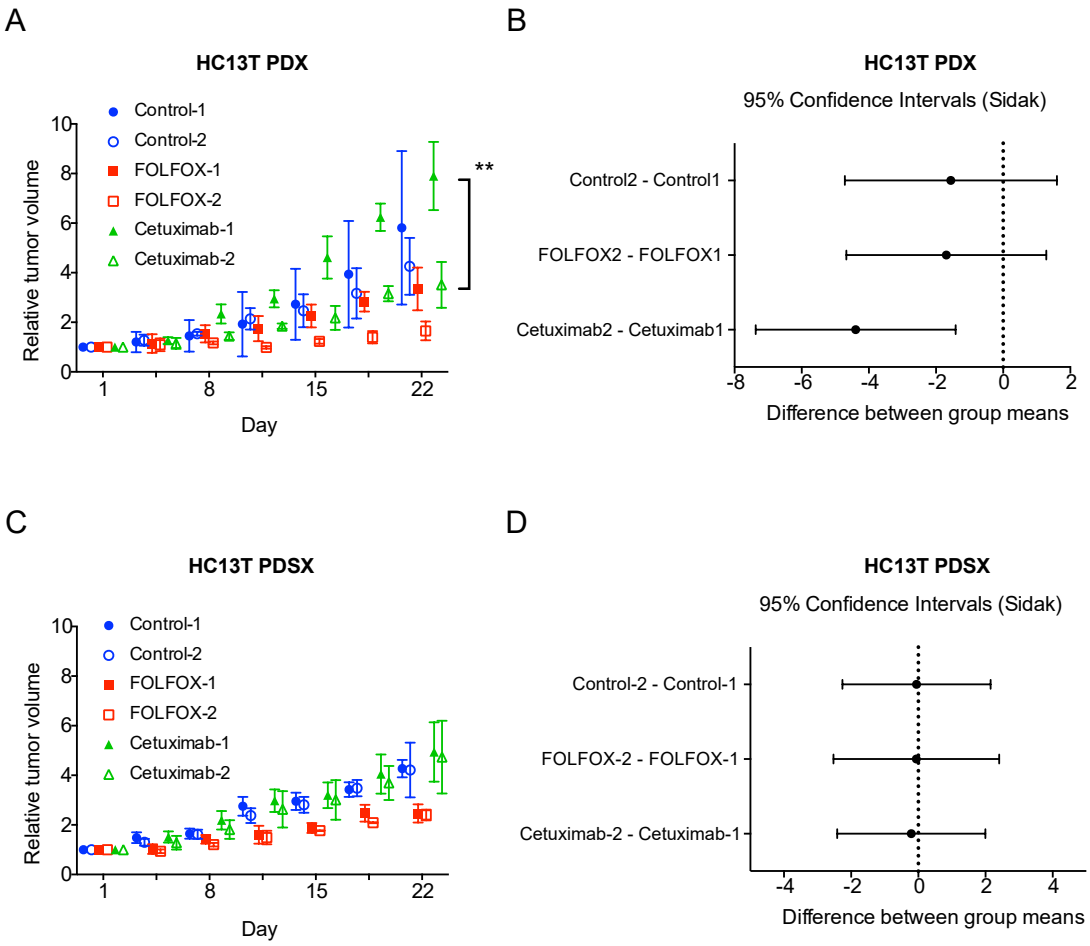

Author Manuscript Published OnlineFirst on July 3, 2018; DOI: 10.1158/1535-7163.MCT-18-0128
Author manuscripts have been peer reviewed and accepted for publication but have not yet been edited.

Figure 3

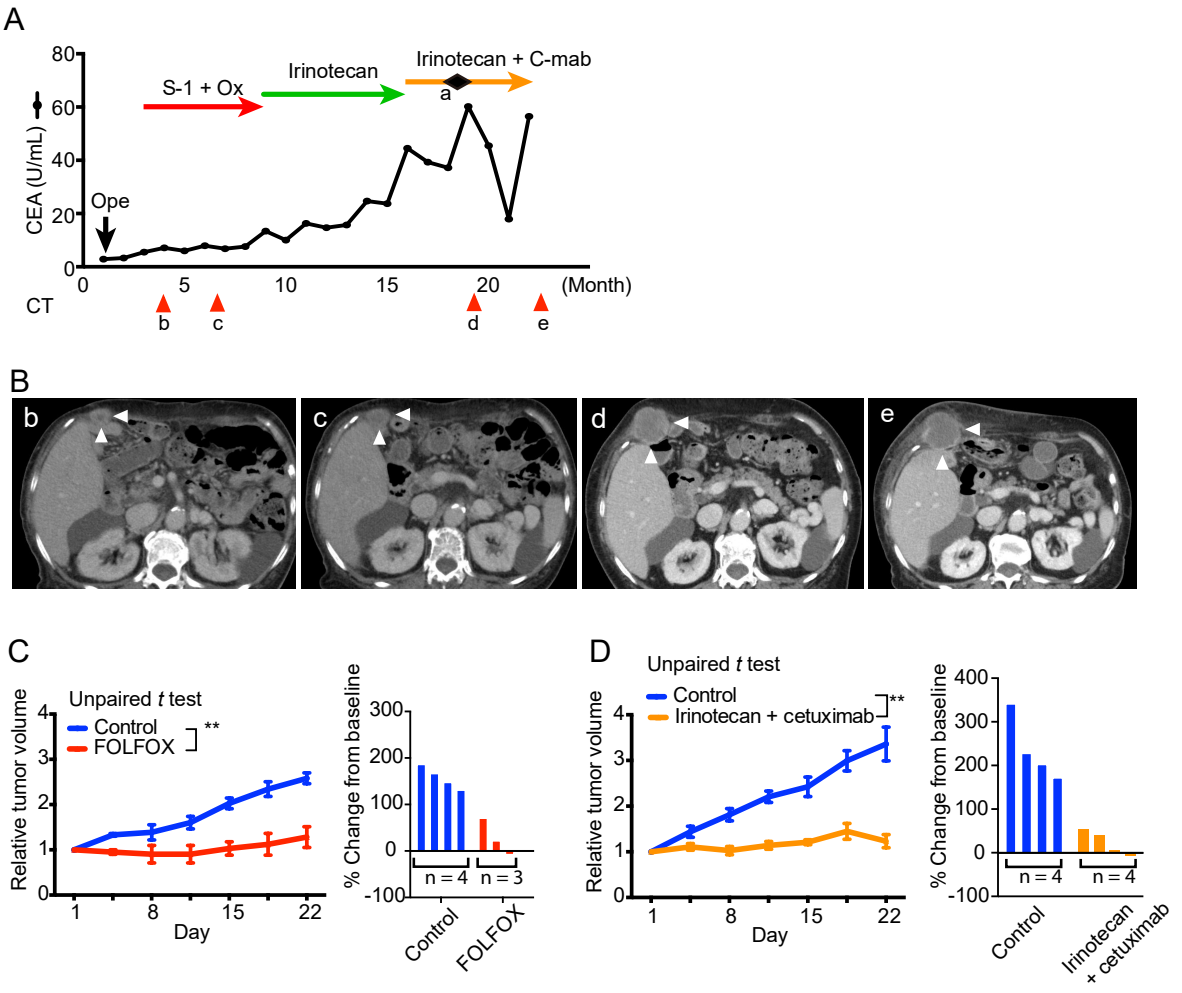

Author Manuscript Published OnlineFirst on July 3, 2018; DOI: 10.1158/1535-7163.MCT-18-0128
Author manuscripts have been peer reviewed and accepted for publication but have not yet been edited.

Figure 4

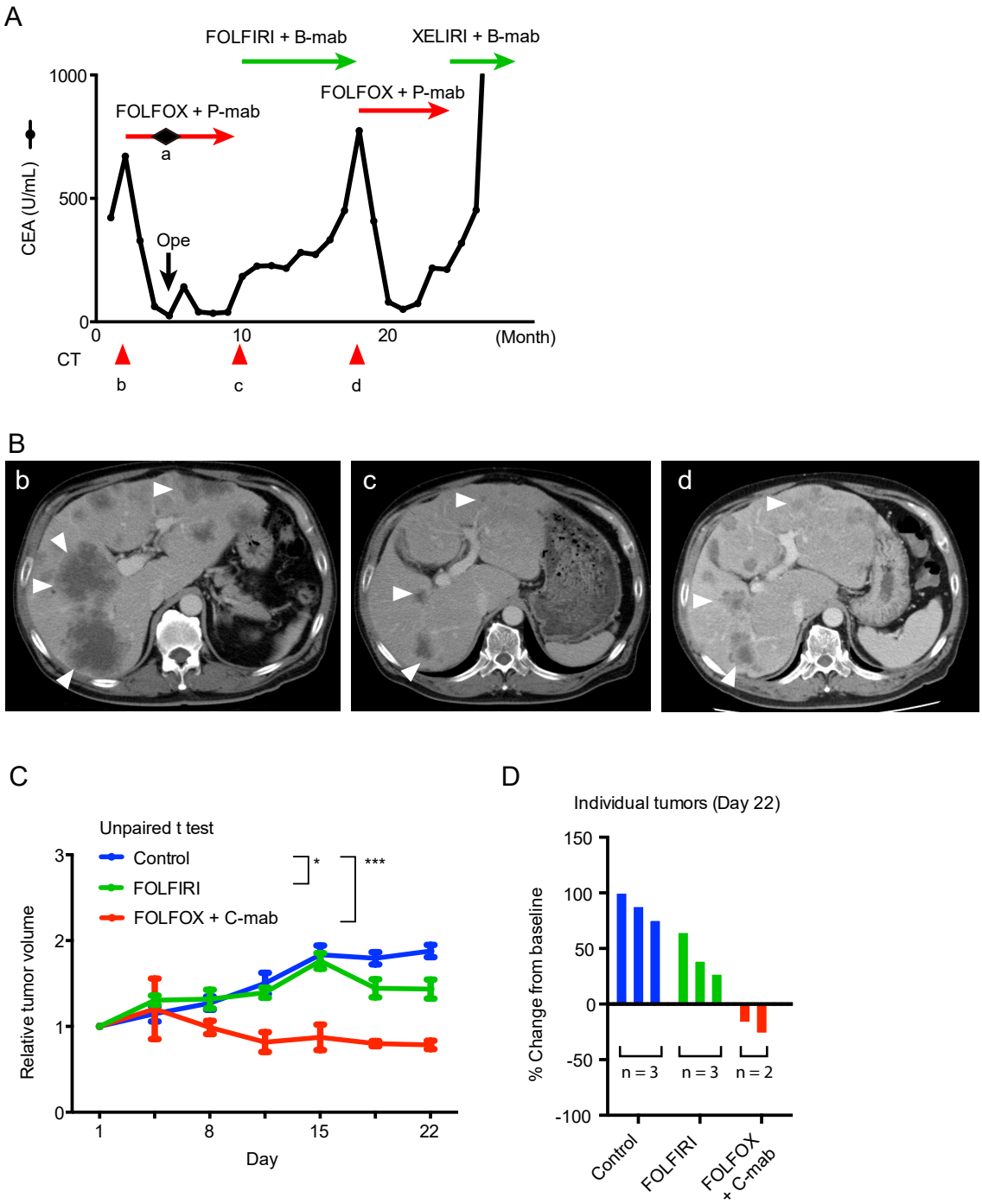

Author Manuscript Published OnlineFirst on July 3, 2018; DOI: 10.1158/1535-7163.MCT-18-0128
Author manuscripts have been peer reviewed and accepted for publication but have not yet been edited.

Figure 5

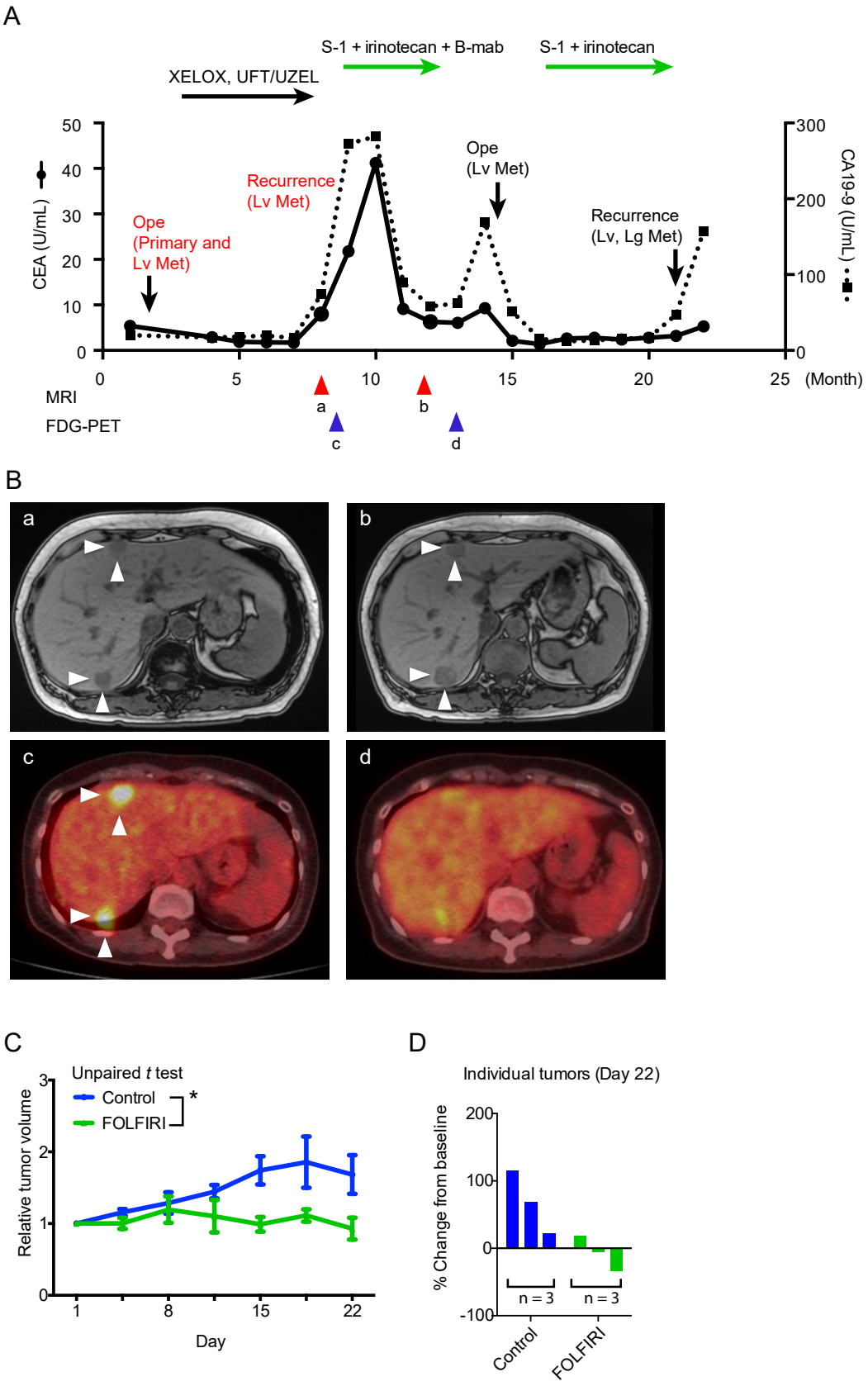

AACR American Association for Cancer Research

Molecular Cancer Therapeutics

A Chemosensitivity Study of Colorectal Cancer Using Xenografts of Patient-Derived Tumor Initiating Cells

Hisatsugu Maekawa, Hiroyuki Miyoshi, Tadayoshi Yamaura, et al.

Mol Cancer Ther Published OnlineFirst July 3, 2018.

Supplementary Table S1. Clinical statuses and success rates for PDXs (P_0) and TIC spheroids (*in vitro*)

	All		PDX				TIC spheroid				
	n = 92		Yes		No		Tumor take rate	Yes		No		Success rate
Total; n, %			56		36		61%	68		24		74%
Age; median, (range)	71 (36–89)		71 (36–89)		70 (39–89)			71 (36–89)		71.5 (44–78)		
Sex; n, %												
Female	38	41%	25	45%	12	33%	68%	28	41%	10	42%	74%
Male	54	59%	31	55%	23	64%	57%	40	59%	14	58%	74%
Stage; n, %												
I	7	8%	2	4%	5	14%	29%	5	7%	2	8%	71%
II	42	46%	24	43%	18	50%	57%	29	43%	13	54%	69%
III	28	30%	20	36%	8	22%	71%	22	32%	6	25%	79%
IV	15	16%	10	18%	5	14%	67%	12	18%	3	13%	80%
Histolog; n, %												
Well - Mod	86	93%	50	89%	36	100%	58%	63	93%	23	96%	73%
Poor	2	2%	2	4%	0	0%	100%	2	3%	0	0%	100%
Mucinous	4	4%	4	7%	0	0%	100%	3	4%	1	4%	75%
Location; n, %												
Right	35	38%	22	39%	13	36%	63%	27	40%	8	33%	77%
Left	33	36%	22	39%	11	31%	67%	24	35%	9	38%	73%
Rectum	24	26%	12	21%	12	33%	50%	17	25%	7	29%	71%
Pre-tratment; n, %												
Yes (chemotherapy)	10	11%	5	9%	5	14%	50%	9	13%	1	4%	90%
No	82	89%	51	91%	31	86%	62%	59	87%	23	96%	72%

Abbreviations: Well - Mod, well- or moderately differentiated adenocarcinoma; Poor, poorly differentiated atenocarcinoma; Mucinous, mucinous adenocarcinoma

Supplementary Table S2. Details of 21 cases of PDSXs

Tumor ID	Patient		Tumor			PDSX	PDX		Mutations in fifty cancer-related genes[a]	MSI/S
	Age	Sex	Location	Histology	Stage		P_0	P_1		
HC1T	81	F	Right	Well - Mod	4	Y	Y	Y	*PIK3CA*	MSS
HC2T	47	M	Right	Well - Mod	3	N	Y	N	*APC*, *KRAS*(G12V)	MSS
HC3T	61	M	Left	Well - Mod	2	Y	Y	Y	*APC*, *KRAS*(G12D)	MSS
HC4T	88	M	Right	Well - Mod	2	Y	Y	Y	[c] *BRAF*, *STK11*, **FGFR3*, **CTNNB1*, **NOTCH1*	MSI
HC5T	63	M	Right	Well - Mod	4	Y	Y	Y	*TP53, PIK3CA,*	MSS
HC6T	57	M	Left	Well - Mod	4	Y	N	–	*TP53*	MSS
HC7T	68	F	Right	Well - Mod	2	Y	N	–	None	MSS
HC8T[b]	66	F	Right	Well - Mod	1	Y	Y	N	[c] **APC, *FBXW7, PIK3CA, ERBB4*, *MLH1*, *SRC*, **ERBB2*, **FLT3*, **CSF1R*, **GNAS*, **JAK3*	MSI
HC10T	70	F	Right	Well - Mod	2	N	N	–	*APC*, *TP53*, *CDH1*	MSS
HC13T	66	M	Left	Poor	3	Y	Y	Y	[c] *BRAF*, *TP53*, **SMAD4*	MSS
HC15T	68	F	Rectum	Well - Mod	3	Y	N		*APC*, *KRAS*(A146T), *FBXW7*	MSS
HC16T	89	M	Left	Well - Mod	3	Y	Y	Y	*TP53*, *FBXW7*	MSS
HC17T	86	M	Right	Well - Mod	3	Y	Y	Y	[c] *APC*, *KRAS*(G12C), *TP53*, *PIK3CA*, *SMAD4*	MSS
HC20T[b]	66	F	Left	Well - Mod	4	Y	Y	N	*TP53*, *SMAD4*, *ERBB4, MLH1*	MSS
HC26T	84	F	Right	Well - Mod	1	Y	Y	Y	[c] *BRAF*, *FBXW7*, *SRC*, **ERBB4*, **FLT3*, **ALK*, **EGFR*	MSI
HC36T	61	F	Left	Well - Mod	3	Y	Y	Y	*APC*, *KRAS*(G12D), *TP53*, *SMAD4*, *CDKN2A*	MSS
HC50T	52	F	Rectum	Well - Mod	4	Y	Y	Y	[c] **APC*, *KRAS*(G12D), *TP53*, **JAK3*	MSS
HC58T	74	M	Left	Well - Mod	4	N	N	–	[c] *APC*, *KRAS*(Q61H), *FBXW7*, **MET*	MSS
HC59T	80	M	Left	Well - Mod	4	Y	Y	Y	[c] **APC*, *KRAS*(G12D), *TP53*	MSS
HC70T	72	F	Right	Mucinous	4	Y	Y	NA	[c] *APC*, *KRAS*(G12D), *FBXW7*, **KDR*	MSS
HC73T	75	M	Left	Well - Mod	4	Y	Y	NA	[c] **APC*, *TP53*, *ERBB2*	MSS
					Take rate (n)	86% (18/21)	76% (16/21)	58% (11/19)		

NOTE: a, fifty cancer-related genes were analyzed by Ion AmpliSeq Cancer Hotspot Panel v2 at Macrogen, Republic of Korea ; b, HC8T and HC20T were derived from the same patient (syncronous double cancers); c, only 50.5% of mutations in the APC gene was detectable due to limited coverage of the panel (based on the COSMIC database; http://cancer.sanger.ac.uk/cosmic) and whole exones were seqenced additionaly to determine out-of-range mutations (asteriscs)

Abbreviations: F, female; M, male; Well - Mod, well- or moderately differentiated adenocarcinoma; Poor, poorly defferentiated adenocarcinoma; Mucinous, mucinous adenocarcinoma; Y, established; N, failed; NA, not available at the time of writing; MSI, microsatellite instable; MSS, microsatellite stable

Supplementary Table S3. Correlations of drug-dosing results between PDSX and PDX methods

		T/C (day 22)		TGI (day 22)	
ID	Treatment	PDX	PDSX	PDX	PDSX
HC13T	FOLFOX	48%	57%	65%	56%
	Cetuximab	120%	114%	-25%	-18%
HC5T	FOLFOX	26%	55%	103%	85%
	Cetuximab	96%	105%	5%	-10%
HC16T	FOLFOX	46%	50%	128%	139%
	Cetuximab	23%	35%	139%	183%
HC17T	FOLFOX	48%	51%	82%	95%
	Cetuximab	50%	36%	73%	126%
Spearman's correlation test		$R = 0.67$		$R = 0.90$	
		$P < 0.05$		$P < 0.01$	

Note: Drug sensitivities in PDSX were very similar to those in PDX. There were statistically significant correlations between PDSX and PDX for both T/C ($R = 0.67$, $P < 0.05$) and TGI ($R = 0.90$, $P < 0.01$).

Supplementary Table S4. Relative tumor volumes and their variances in drug-dosing tests for PDSX and PDX (Day 22)

		PDSX			PDX			
	Group	Relative Tumor Volume	SD	CV (%)	Relative Tumor Volume	SD	CV (%)	
HC13T	Control	4.2	0.7	17	4.8	1.8	38	
	FOLFOX	2.4	0.3	12	2.3	1.1	46	
	Cetuximab	4.8	1.2	25	5.7	2.4	42	
HC5T	Control	2.2	0.1	4	3.6	1.2	34	
	FOLFOX	1.2	0.4	37	0.9	0.3	35	
	Cetuximab	2.3	0.4	17	3.5	1.1	31	
HC16T (1st set)	Control	1.6	0.4	24	1.7	0.2	13	
	FOLFOX	0.8	0.1	11	0.8	0.4	53	
	Cetuximab	0.5	0.2	32				
HC16T (2nd set)	Control				2.3	0.6	28	
	FOLFOX							
	Cetuximab				0.5	0.1	11	
HC17T (1st set)	Control	2.0	0.3	16	2.7	0.8	31	
	FOLFOX	1.0	0.2	16	1.3	0.5	39	
	Cetuximab	0.7	0.1	15				
HC17T (2nd set)	Control				3.2	0.7	21	
	FOLFOX							
	Cetuximab				1.6	0.3	17	
Mean				19			31	$P < 0.01$ [a]

Abbreviations: SD, standard deviation; CV, coefficient of variation

Note: a, there was a significant difference between the mean value of CVs in PDSX and that in PDX for unpaired *t* test with Welch's correction.

Supplementary Table S5. Patient outcome and drug sensitivity with PDSXs

Tumor ID	Patient				PDSX			
	Chemotherapy	RECIST (BR)	CEA level	DOR	Chemotherapy	T/C	TGI	Significance[c]
HC1T	SOX	SD (11%)	stable	4	FOLFOX	50%	82%	+
	Irinotecan + C-mab	SD (3%)	decreased	6	Irinotecan + C-mab	37%	93%	+
HC5T	Irinotecan	N.A. (PD)[a]	increased	0	Irinotecan	82%	30%	-
HC6T	FOLFOX + C-mab	PR (-60%)	decreased	9	FOLFOX + C-mab	42%	122%	+
	FOLFIRI + B-mab	SD (10%)	stable	5	FOLFIRI	76%	50%	+
HC50T	IRIS+B-mab	PD (21%)[b]	decreased	4	FOLFIRI	55%	107%	+
HC59T	FOLFOX + B-mab	SD (-24%)	decreased	NA	FOLFOX	61%	128%	+
HC70T	FOLFOX + B-mab	SD (-27%)	stable	NA	FOLFOX	42%	79%	+
HC73T	FOLFOX + C-mab	PR (-55%)	decreased	8	FOLFOX + C-mab	13%	131%	+

NOTE: a, assessed as PD by clinical course; b, assessed as PD by MRI, although the results of ^{18}F-FDG-PET showed discrepancy (see text); c, +, $P < 0.05$, -, $P \geq 0.05$ by unpaired *t*-test or Tukey's multiple comparisons test in PDSX dosing tests

Abbreviations: BR, best response with RECIST; DOR, duration of response; SOX, S-1 + oxaliplatin; C-mab, cetuximab; B-mab, bevacizumab, IRIS, irinotecan + S-1; SD, stable disease; PR, partial response; PD, progressive disease; NA, not available

Supplementary figure S1

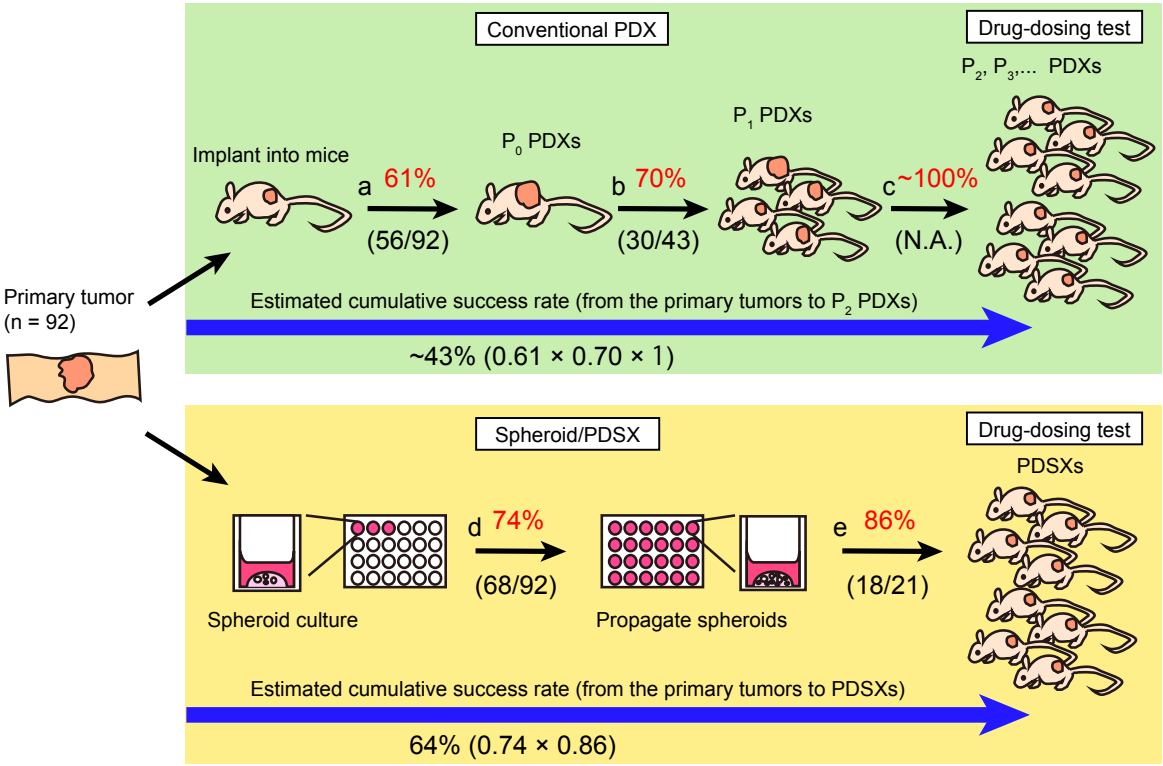

Supplementary Figure S1.
Mouse preparation efficiencies for drug sensitivity tests with PDXs (top) and PDSXs (bottom). Black arrows (a–e) show the following steps; establishment of P_0 PDXs from patient tumors (a), passaging and formation of P_1 PDXs from P_0 PDX tumors (b), preparation of P_2 PDXs from P_1 PDXs (c), establishment of spheroids from patient tumors (d), and formation of PDSXs from spheroids (e). The percentages show success rates at the respective steps whereas the numbers indicate (succeeded/tried) mice. Blue arrows indicate estimated cumulative success rates for PDXs (top; from primary tumors to P_2 PDXs) and PDSXs (bottom; from primary tumors to PDSXs).

Supplementary figure S2

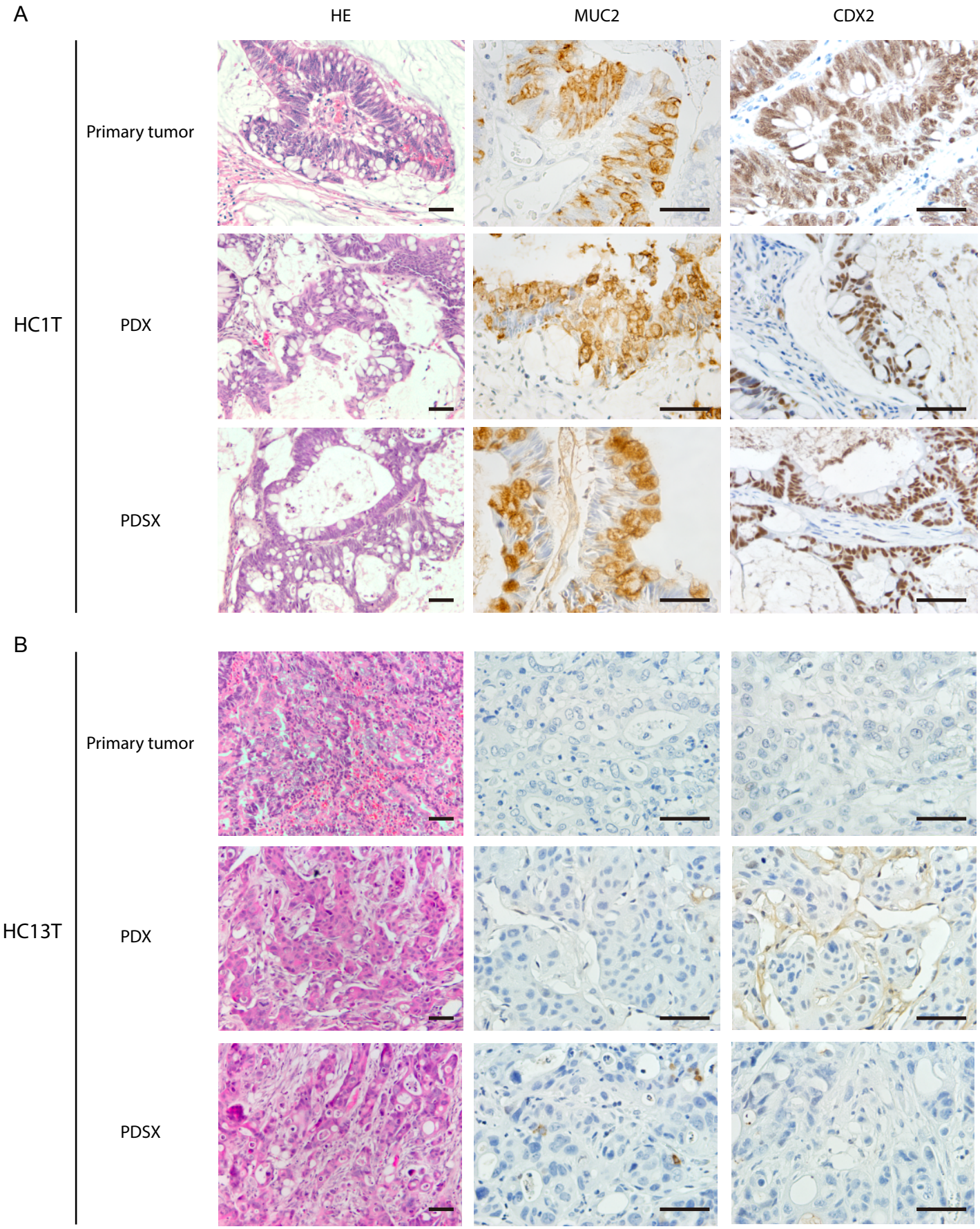

Supplementary figure S2

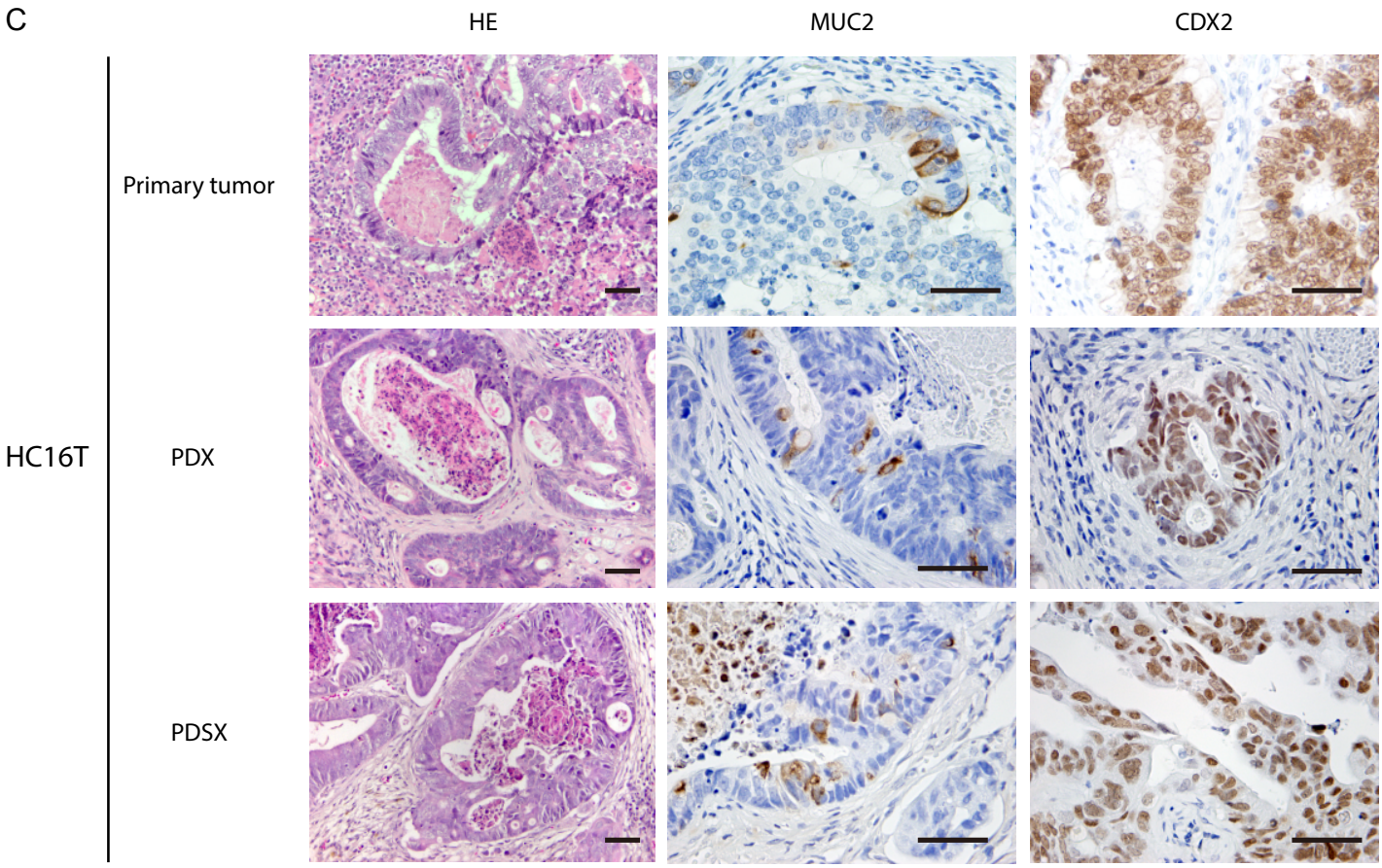

Supplementary Figure S2.
Histopathology of the primary (top), PDX (middle), and PDSX (bottom) tumors analyzed by H&E staining (left), and by IHC for MUC2 (center) and CDX2 (right). A, Histopathology of HC1T. In H&E staining (left), all three samples contained many goblet cells and cancer epithelial cells surrounded by mucus. Goblet cells were also confirmed by IHC for MUC2 (center). CDX2 expression was also detected by IHC (right). **B**, Histopathology of HC13T. In H&E staining (left), all three samples showed poorly differentiated adenocarcinoma. IHC for MUC2 (middle) or CDX2 (right) had no stained epithelial cells. **C**, Histopathology of HC16T. In H&E staining (left), all three samples consisted of well–moderately differentiated adenocarcinoma with some necrosis. MUC2 staining (center) revealed only a few goblet cells. Note that all PDSX tumors retained the epithelial characteristics of the corresponding primary tumors of the patients whereas most stromal cells derived from the host mice. Magnification bar, 50 μm.

.

Supplementary figure S3

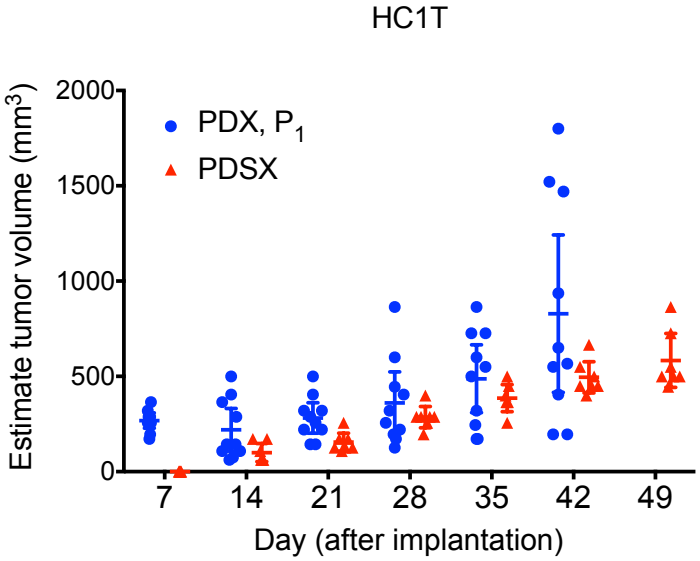

Supplementary Figure S3.
Growth of the xenograft tumors as PDXs and PDSXs derived from the same cancer (HC1T). Each data point shows the estimated volume for each PDX (blue) or PDSX (red) tumor. Error bars show SDs. To help visual clarity, three data points for each day were aligned horizontally, avoiding their superimposition. Accordingly, both blue (for PDX, P_1) and red (for PDSX) points are slightly off the center although they represent precisely the same day.

Supplementary figure S4

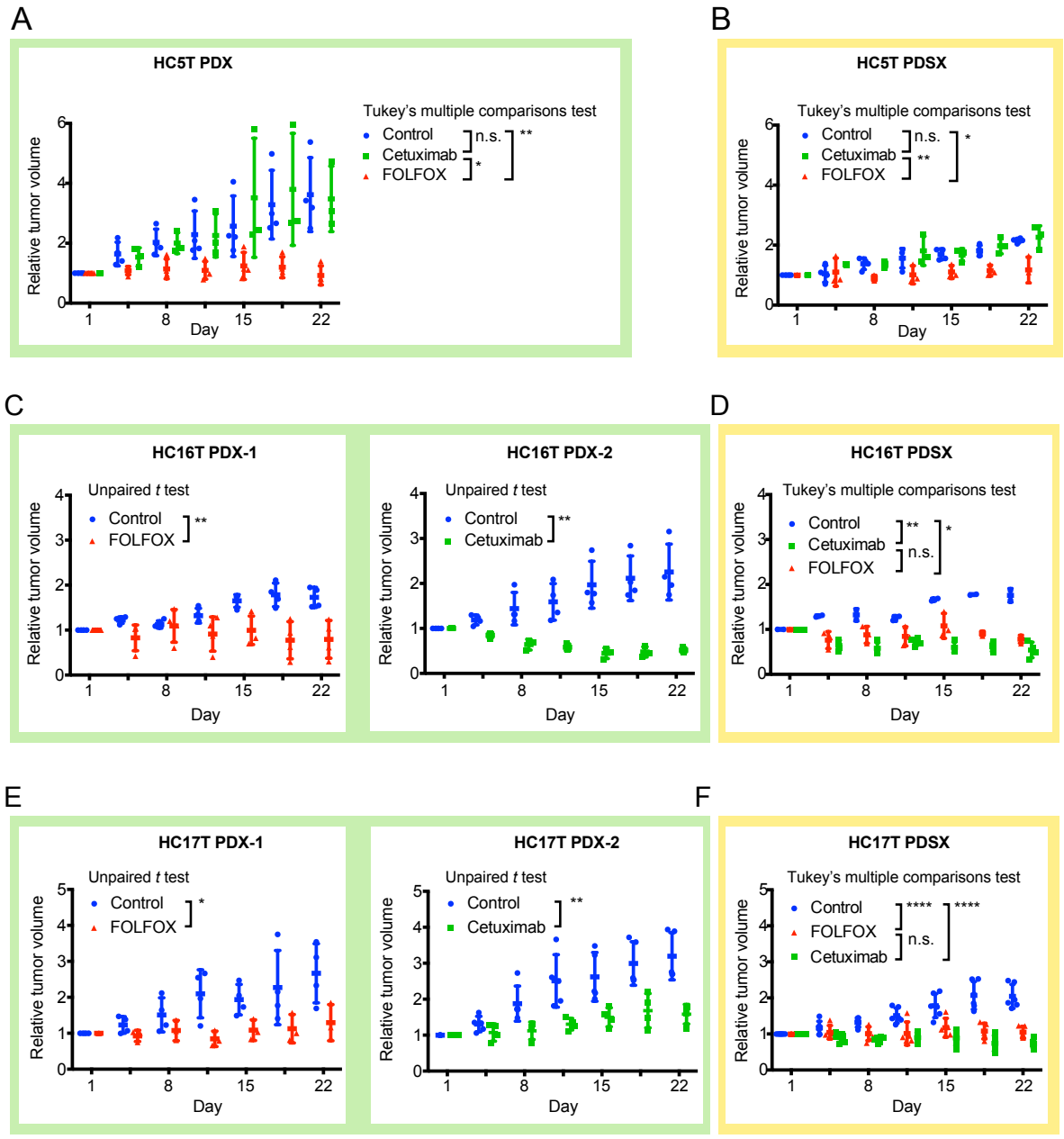

Supplementary Figure S4.
Comparison between PDXs and PDSXs in drug-dosing tests (with HC5T, HC16T, and HC17T). **A** and **B**, Results of drug-dosing tests with HC5T PDXs (A) and PDSXs (B). **C** and **D**, Those with HC16T PDXs (C) and PDSXs (D). **E** and **F**, Those with HC17T PDXs (E) and PDSXs (F). The PDX-1 and PDX-2 were derived from small fragments of the same subregion of a tumor, and were the first (control vs. FOLFOX) and second (control vs. cetuximab) sets of drug-dosing tests, respectively. For preparation of the second set, additional passages of PDX tumors were performed. Each data point shows the tumor volume of each PDX/PDSX on day x relative to that of day 1. ($n = 3$–4 in each group; Error bars show SDs. *, $P < 0.05$; **, $P < 0.01$; and ****, $P < 0.0001$ in unpaired *t* test or Tukey's multiple comparison test). To help visual clarity, two or three data points for each day were aligned horizontally, avoiding their superimposition. Accordingly, some of the points are slightly off the center although they all represent precisely the same day.

Supplementary figure S5

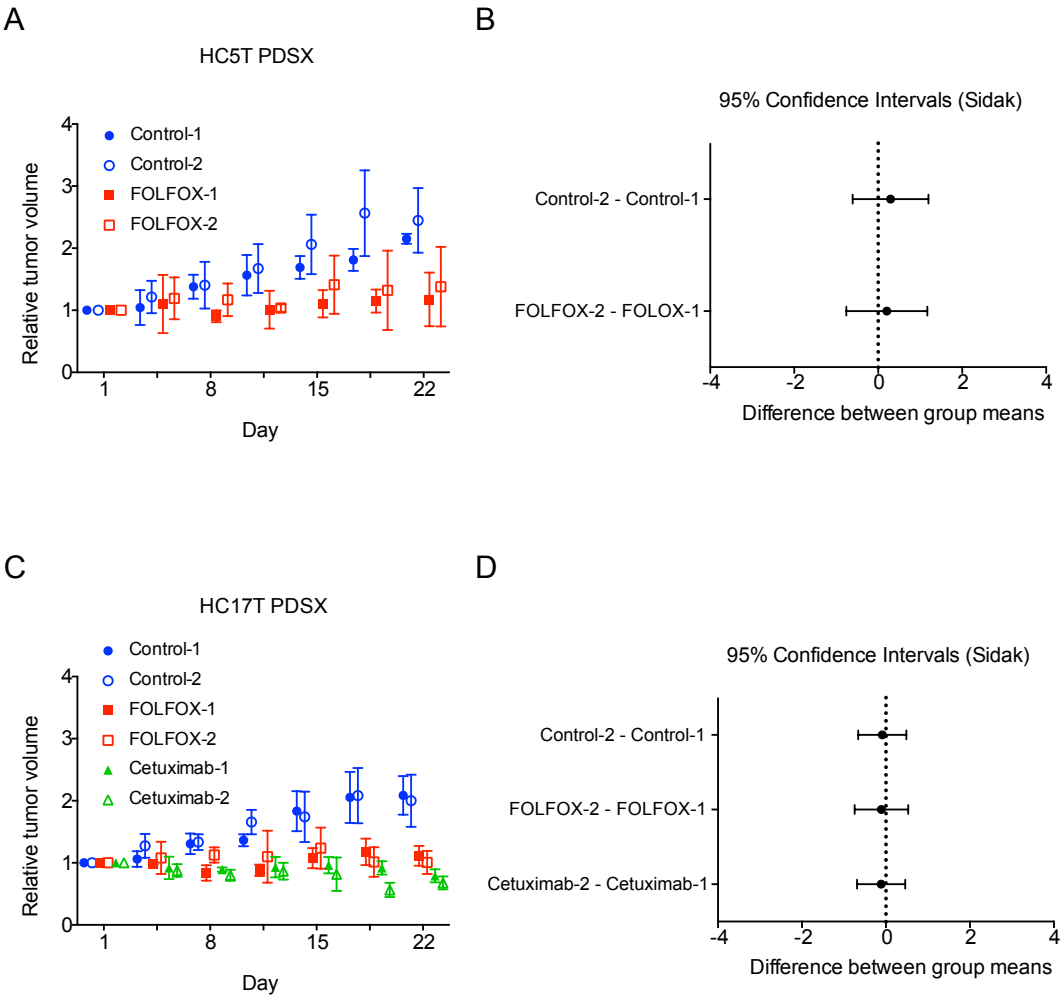

Supplementary Figure S5.
Reproducibility of PDSXs in drug dosing tests (with HC5T and HC17T). A, Results from the first (filled symbols) and second (open symbols) rounds of drug-dosing tests with HC5T PDSX mice. (n = 3–4 in each group). PDSXs derived from P_8 and P_{18} spheroids were used for the first and second round, respectively. **B**, Result of Sidak's multiple comparison test for the corresponding groups in two rounds of dosing tests with HC5T PDSXs (e.g., difference between Control-1 and Control-2). **C**, Results from the first (filled symbols) and second (open symbols) rounds of drug-dosing tests with HC17T PDSX mice (n = 2–3 in each group). P_6 and P_{11} generation PDSX mice were used for the first and second rounds, respectively. **D**, Result of Sidak's multiple comparison test for the corresponding groups in two rounds of dosing tests with HC17T PDSXs. To help visual clarity, four data points for each day in (A) and (C) were aligned horizontally, avoiding their superimposition. Accordingly, some of the points are slightly off the center although they all represent precisely the same day.

Supplementary Figure S6

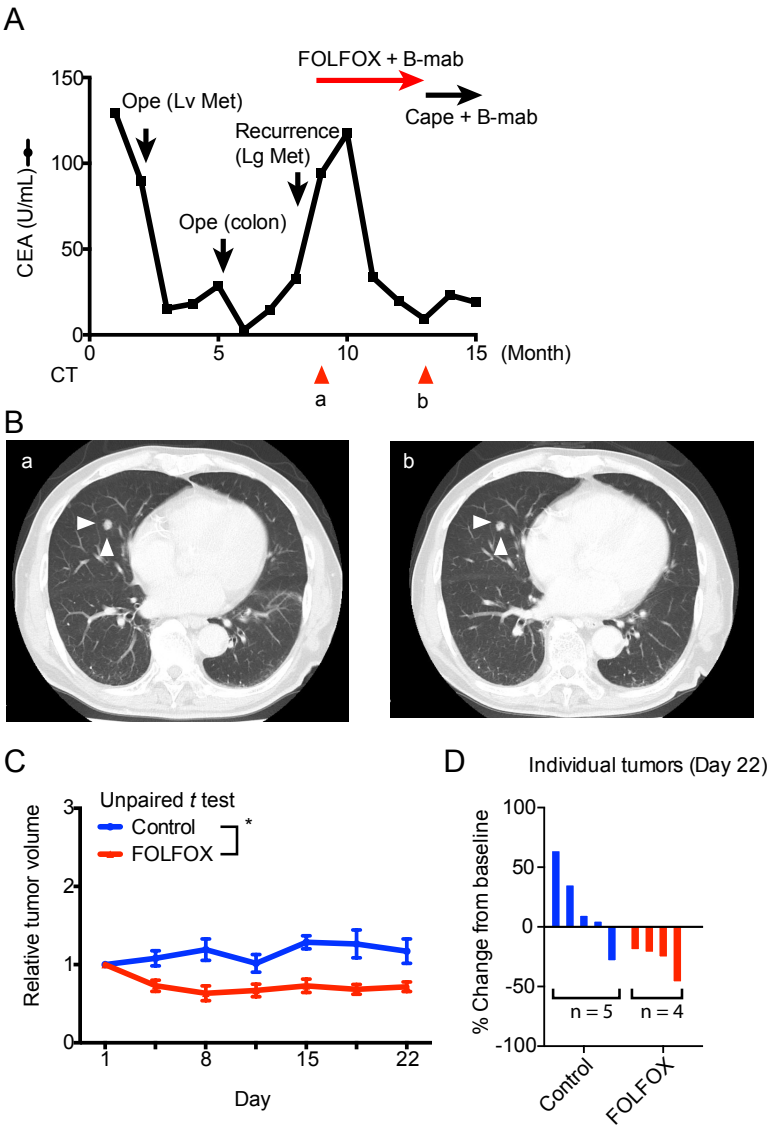

Supplementary Figure S6.
Clinical course of the patient during the chemotherapy who had colon cancer HC59T, and its drug responses as PDSXs. The patient received FOLFOX + bevacizumab, which resulted in SD for 3 months. To reduce the adverse effects, FOLFOX was then replaced with capecitabine (DOR; not available because the treatment was terminated before becoming resistant due to adverse effects). Regarding the PDSX mice treated with FOLFOX, tumors showed moderate response with a significant difference from the control. The clinical response of this patient to FOLFOX was reproduced in the PDSX model.

A, The serum CEA level was monitored. Chemotherapy regimens given to the patient are shown on top with arrows that indicate the durations. Ope, operation; Lv, liver; Lg, lung; Met, metastasis; B-mab, bevacitumab. The red arrowheads (a and b) indicate the timing of CT assessments in (B). **B**, CT images of the patient lungs before (a) and after (b) FOLFOX + B-mab treatment. White arrowheads point to a metastatic tumor. The best response to FOLFOX + B-mab treatment in the patient was SD (-24%). **C**, Drug-dosing tests of PDSXs derived from the primary colon cancer. The tumor growth in FOLFOX group was significantly decreased compared with that in control. (T/C = 61%, TGI = 128%, *, $P < 0.05$, unpaired *t* test on day 22. $n = 5$ and 4 in control and FOLFOX groups, respectively. Error bars show SEMs.) **D**, Percent change in tumor volume from individual PDSX mice with or without the dosing (days 1–22).

Supplementary Figure S7

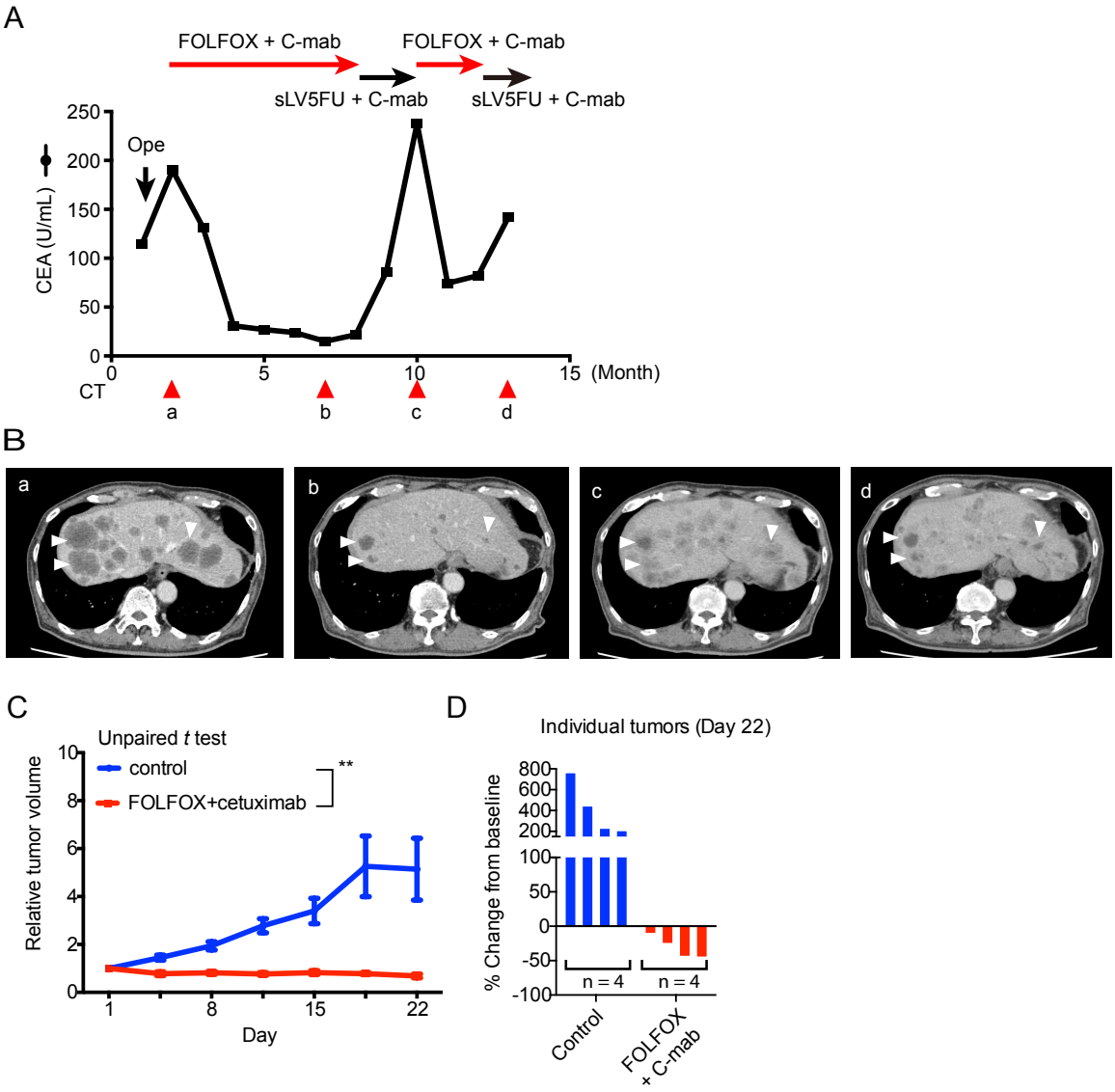

Supplementary Figure S7.
Clinical course of the patient during the chemotherapy who had colon cancer HC73T, and its drug responses as PDSXs. This patient received FOLFOX + cetuximab to treat liver metastatic lesions after resection of the primary tumor. The treatment resulted in PR for 8 months. The PDSX mice carrying his primary tumors were treated with FOLFOX + cetuximab regimen that also caused PR.

A, The CEA level was monitored. Chemotherapy regimens given to the patient are shown on top with colored arrows that indicate the durations. C-mab, cetuximab. The red arrowheads (a, b, c, and d) indicate the timing of CT assessments in (B). **B**, CT images of the patient liver before (a) and after (b) the first FOLFOX + C-mab treatment, followed by those before the second FOLFOX + C-mab (c) and after the second aLV5FU + C-mab (d). White arrowheads point to representative metastatic tumors. The best response to FOLFOX + C-mab treatment in the patient was PR (-55%). **C**, Drug-dosing tests with PDSXs derived from the patient tumor HC73T. The tumor growth in the FOLFOX + C-mab group was significantly inhibited compared with that in the control group. (T/C = 13%, TGI = 131%, **, $P < 0.01$, unpaired t test on day 22. $n = 4$ in each group. Error bars show SEMs.) **D**, Percent changes in tumor volume from the individual PDSX mice with or without the dosing (days 1–22).

Supplementary Figure S8

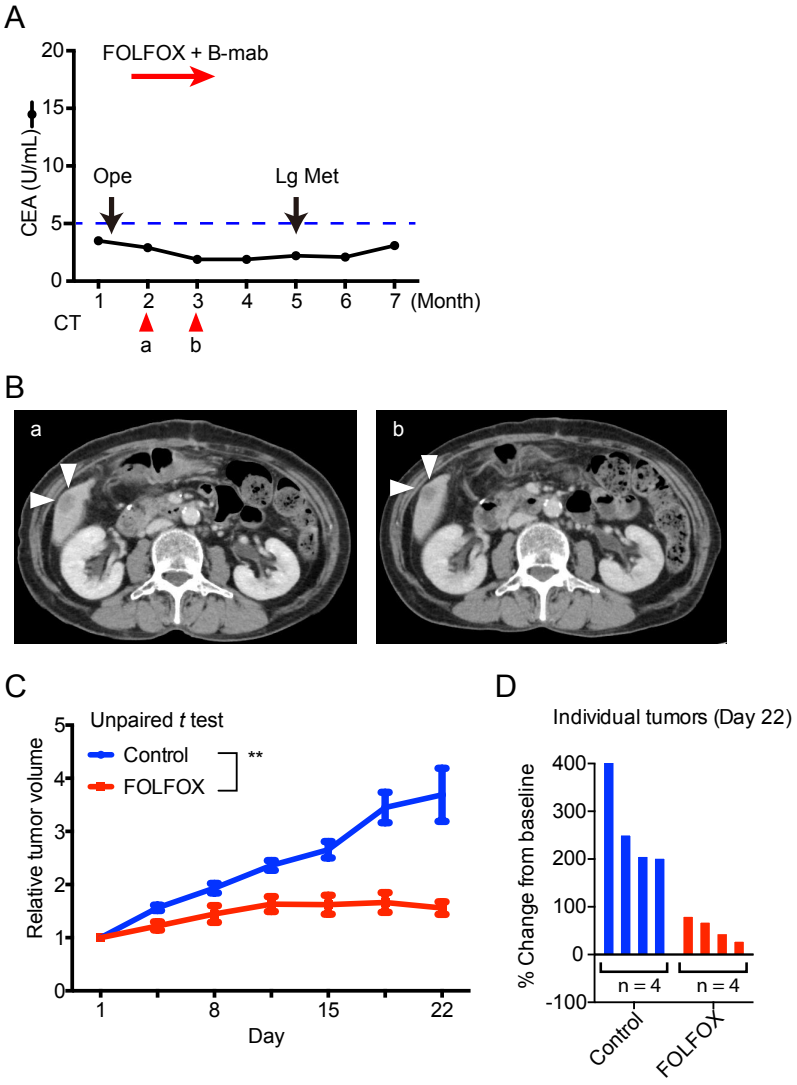

Supplementary Figure S8.
Clinical course of the patient during the chemotherapy who had colon cancer HC70T, and its drug response as PDSXs. This patient was received FOLFOX + bevacizumab treatment that led to SD for 2 months. However, she complained severe fatigue by the treatment and decided to discontinue further chemotherapies (DOR; not available). The clinical response of this patient to FOLFOX was reproduced in the PDSX model.

A, The CEA level did not increase above the normal range (< 5 U/mL). The chemotherapy regimen given to the patient is shown on top with a red arrow that indicate the duration. B-mab, bevacizumab. The red arrowheads (a and b) indicate the timing of CT assessments in (B). **B**, CT images of the patient liver before (a) and after (b) FOLFOX + B-mab treatment. White arrowheads point to a liver metastatic lesion. The best response to FOLFOX + B-mab treatment in the patient was SD (-27%). **C**, Drug-dosing tests with PDSXs derived from the patient tumor HC70T. The tumor growth in the FOLFOX group was significantly inhibited compared with that in the control group. (T/C = 42%, TGI = 79%, **, $P < 0.01$, unpaired *t* test on day 22. $n = 4$ in each group. Error bars show SEMs.) **D**, Percent changes in tumor volume from the individual PDSX mice with or without the dosing (days 1–22).

Supplementary Figure S9

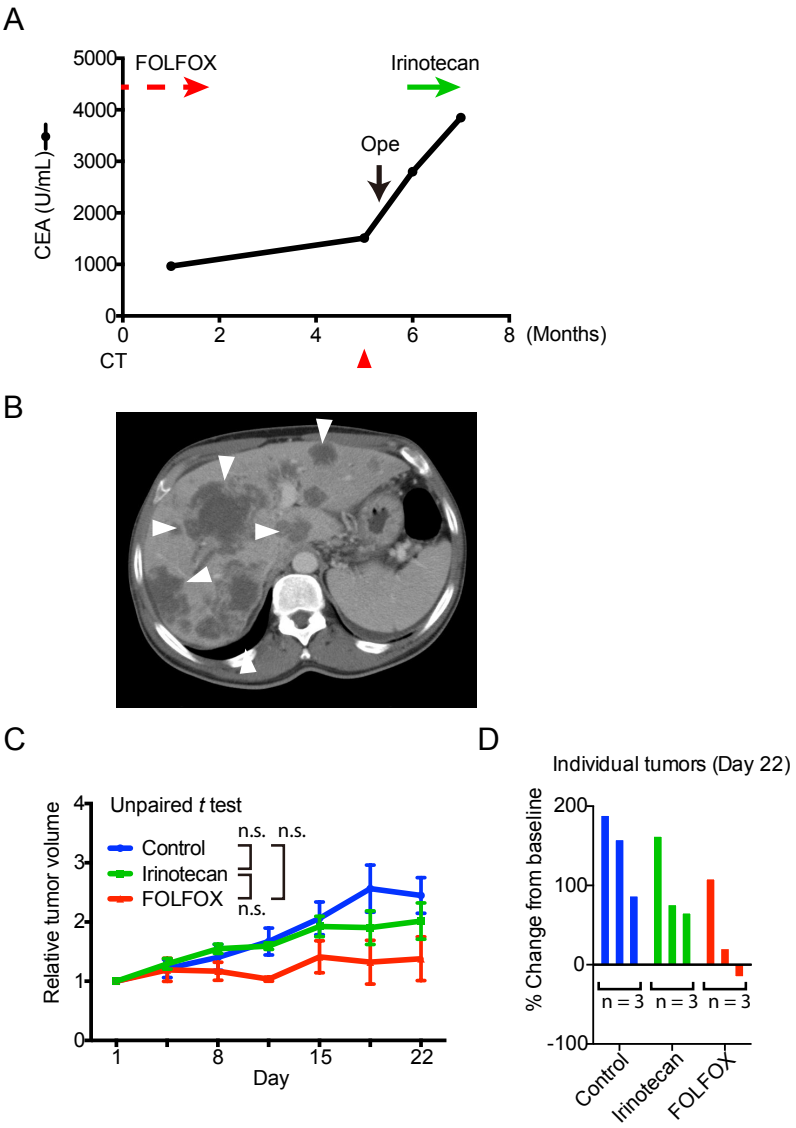

Supplementary Figure S9.
Clinical course of the patient during chemotherapy who had colon cancer HC5T, and its drug response as PDSXs. This patient was treated with irinotecan monotherapy (80% of full dose) as an adjuvant chemotherapy. Unfortunately, the treatment was ineffective, and his colorectal cancer caused a rapid elevation of the serum CEA level, accompanied with liver failure due to massive liver metastatic lesions (PD, DOR; 0 month). The clinical response of this patient to irinotecan was reproduced in the PDSX model.

A, The serum CEA level was monitored. Chemotherapy regimens given to the patient are shown on top with colored arrows that indicate the durations. Ope, operation. The red arrowhead at the bottom indicates the timing of CT assessment in (B). **B**, The CT image of patient liver before the irinotecan treatment. White arrowheads point to representative metastatic regions. (CT examination was not performed after the irinotecan treatment.) **C**, Drug-dosing tests with PDSXs derived from the primary tumor. The PDSXs in irinotecan mice continued to grow, showing only a delayed and slight suppression (T/C = 82%, TGI = 30%). On the other hand, FOLFOX appeared to be effective (T/C = 55%, TGI = 74%), although the difference from control did not reach statistical significance. (n.s., not significant, unpaired *t* test on day 22. $n = 3$ in each group. Error bars show SEMs.) **D**, Percent changes in tumor volume from individual PDSX mice with or without the dosing (days 1–22)

Supplementary figure S10

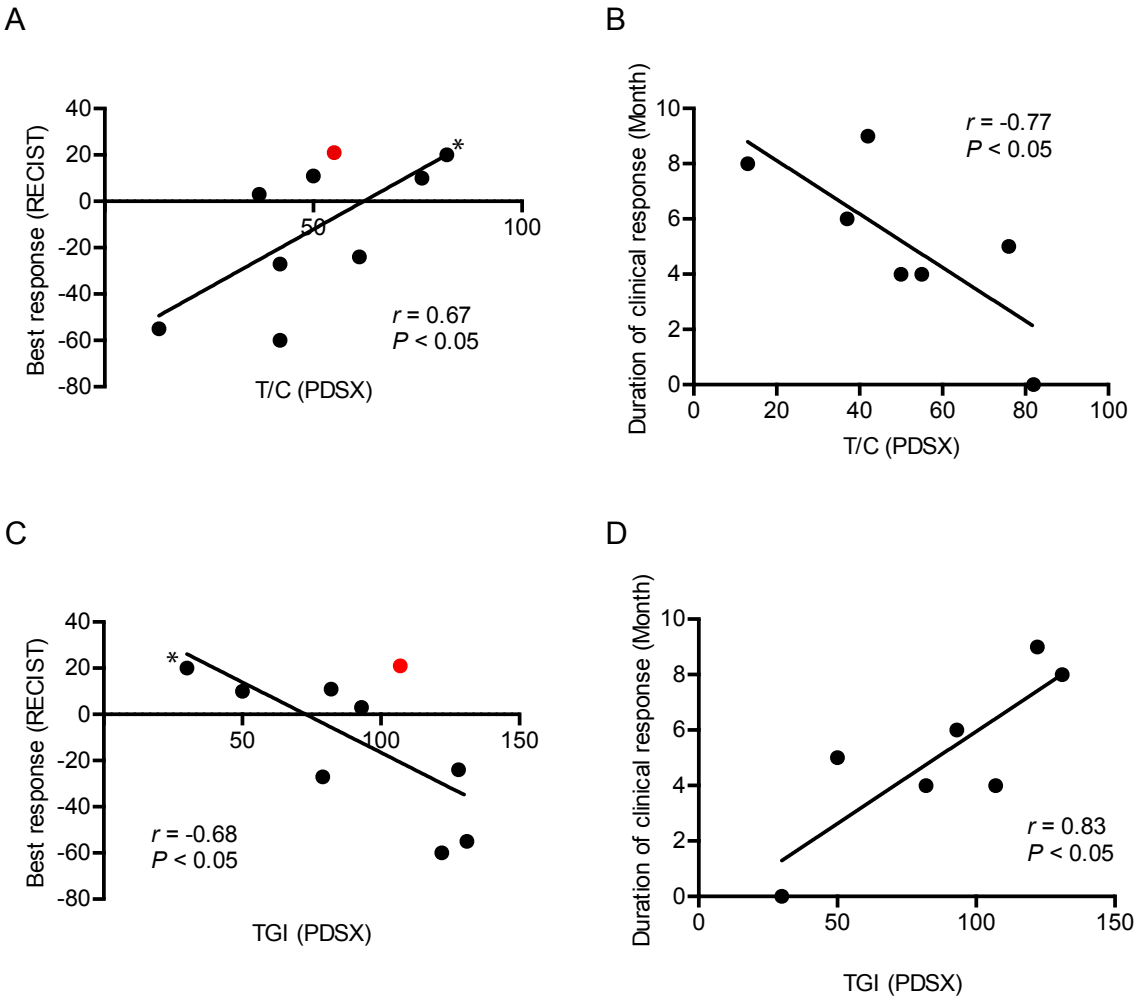

Supplementary figure S10.
Correlations of the PDSX dosing data (T/C and TGI values) with the patients' clinical responses. **A**, Pearson's correlation analysis of the PDSX T/C values and patients' best responses ($r = 0.67$, $P < 0.05$). **B**, Pearson's correlation analysis of the T/C values and the durations of clinical response (DOR) ($r = -0.77$, $P < 0.05$). **C**, Pearson's correlation analysis of the PDSX TGI values and patients' best responses ($r = -0.68$, $P < 0.05$). **D**, Pearson's correlation analysis of the TGI values and the durations of clinical response (DOR). ($r = 0.83$, $P < 0.05$). *, Best response in this particular case was not available, and was preseumed as 20% (the least value of PD) because the treatment effect was assessed as PD (see Patient 7; Supplementary Fig. S9). The red points indicate the only case (Patient 3) that showed an apparent discrepancy between the PDSX drug response and best clinical response in RECIST (see text). If these data points are excluded, the statistical values are: (A, $r = 0.70$, $P = 0.05$), and (C, $r = -0.82$, $P < 0.05$).

Supplementary figure S11

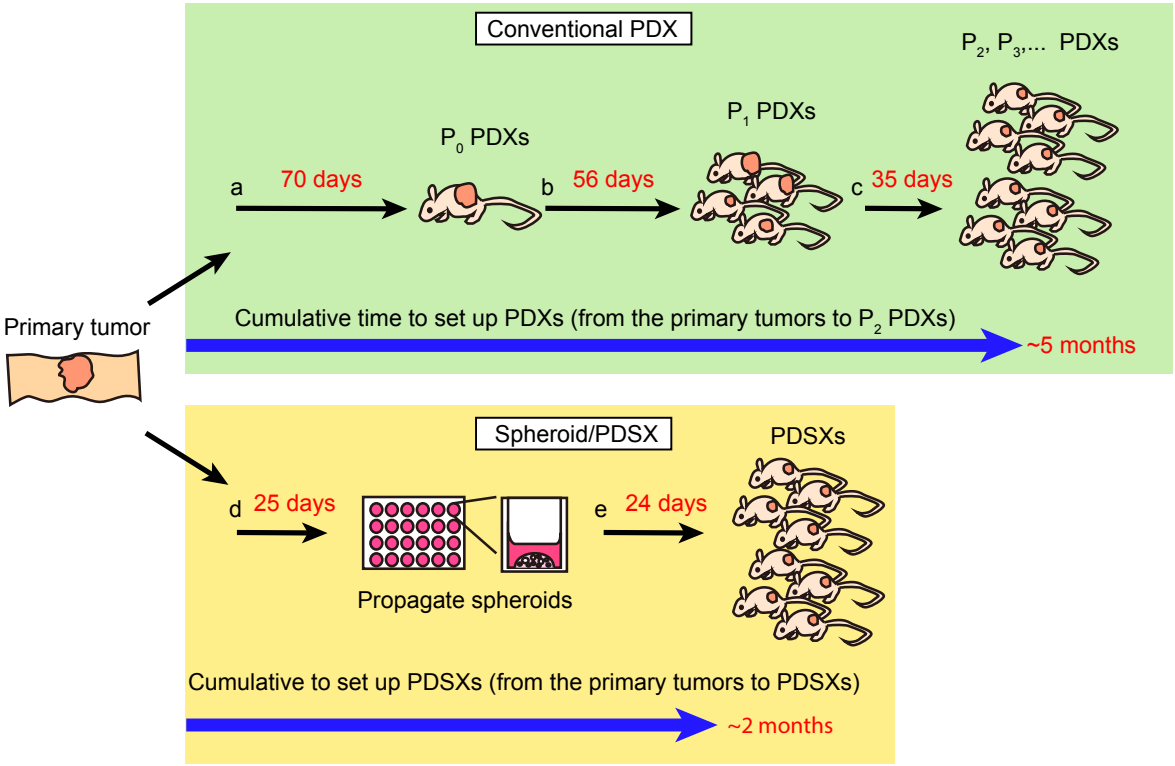

Supplementary Figure S11.
Time line comparison in preparation of the drug-dosing test-mice that carried PDXs (top) and PDSXs (bottom). The "days" above the black arrows indicate the median durations for the respective steps. Blue arrows indicate the cumulative time estimated to set up PDXs (from the primary tumor to P_2 PDXs) and PDSXs (from the primary tumor to PDSXs).